NUCLEAR DATA AND MEASUREMENTS SERIES

ANL/NDM-17

Sample-Size Effects in Fast-Neutron Gamma-Ray Production Measurements: Solid-Cylinder Samples

by

Donald L. Smith

September 1975

ARGONNE NATIONAL LABORATORY,
ARGONNE, ILLINOIS 60439, U.S.A.

NUCLEAR DATA AND MEASUREMENTS SERIES

ANL/NDM-17

SAMPLE-SIZE EFFECTS IN FAST-NEUTRON GAMMA-RAY PRODUCTION MEASUREMENTS: SOLID-CYLINDER SAMPLES

by

Donald L. Smith

September 1975

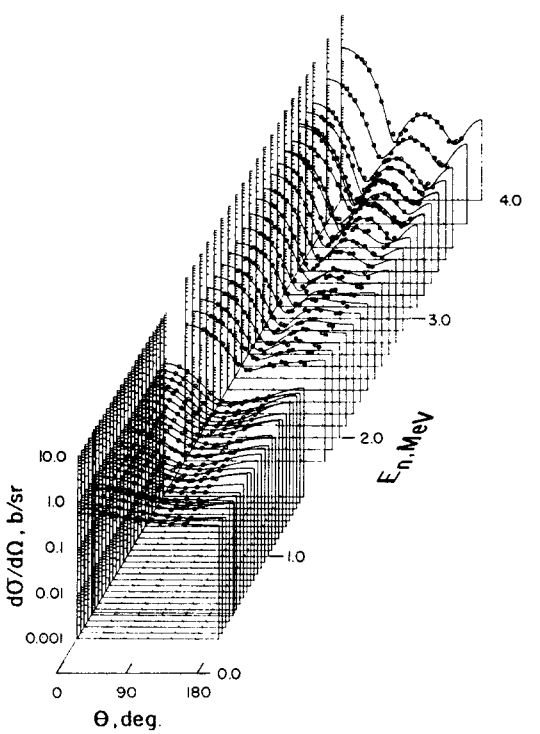

UofC - AUA - USAEC

ARGONNE NATIONAL LABORATORY,
ARGONNE, ILLINOIS 60439, U.S.A.

The facilities of Argonne National Laboratory are owned by the United States Government. Under the terms of a contract (W-31-109-Eng-38) between the U. S. Atomic Energy Commission, Argonne Universities Association and The University of Chicago, the University employs the staff and operates the Laboratory in accordance with policies and programs formulated, approved and reviewed by the Association.

MEMBERS OF ARGONNE UNIVERSITIES ASSOCIATION

The University of Arizona
Carnegie-Mellon University
Case Western Reserve University
The University of Chicago
University of Cincinnati
Illinois Institute of Technology
University of Illinois
Indiana University
Iowa State University
The University of Iowa
Kansas State University
The University of Kansas
Loyola University
Marquette University
Michigan State University
The University of Michigan
University of Minnesota
University of Missouri
Northwestern University
University of Notre Dame
The Ohio State University
Ohio University
The Pennsylvania State University
Purdue University
Saint Louis University
Southern Illinois University
The University of Texas at Austin
Washington University
Wayne State University
The University of Wisconsin

ANL/NDM-17

SAMPLE-SIZE EFFECTS IN FAST-NEUTRON GAMMA-RAY PRODUCTION MEASUREMENTS: SOLID-CYLINDER SAMPLES

by

Donald L. Smith

September 1975

In January 1975, the research and development functions of the former U.S. Atomic Energy Commission were incorporated into those of the U.S. Energy Research and Development Administration.

Applied Physics Division
Argonne National Laboratory
9700 South Cass Avenue
Argonne, Illinois 60439
U.S.A.

NUCLEAR DATA AND MEASUREMENTS SERIES

The Nuclear Data and Measurements Series presents results of studies in the field of microscopic nuclear data. The primary objective is the dissemination of information in the comprehensive form required for nuclear technology applications. This Series is devoted to: a) Measured microscopic nuclear parameters, b) Experimental techniques and facilities employed in data measurements, c) The analysis, correlation and interpretation of nuclear data, and d) The evaluation of nuclear data. Contributions to this Series are reviewed to assure technical competence and, unless otherwise stated, the contents can be formally referenced. This Series does not supplant formal journal publication but it does provide the more extensive information required for technological applications (e.g., tabulated numerical data) in a timely manner.

TABLE OF CONTENTS

SAMPLE-SIZE EFFECTS IN FAST-NEUTRON GAMMA-RAY PRODUCTION MEASUREMENTS: SOLID-CYLINDER SAMPLES*

by

Donald L. Smith

Argonne National Laboratory, Argonne, Illinois 60439, U.S.A.

ABSTRACT

The effects of geometry, absorption and multiple scattering in $(n,X\gamma)$ reaction measurements with solid-cylinder samples are investigated. Both analytical and Monte-Carlo methods are employed in the analysis. Geometric effects are shown to be relatively insignificant except in definition of the scattering angles. However, absorption and multiple-scattering effects are quite important; accurate microscopic differential cross sections can be extracted from experimental data only after a careful determination of corrections for these processes. The results of measurements performed using several natural iron samples (covering a wide range of sizes) confirm validity of the correction procedures described herein. It is concluded that these procedures are reliable whenever sufficiently accurate neutron and photon cross section and angular distribution information is available for the analysis.

*This work was performed under the auspices of the U.S. Energy Research and Development Administration.

1. INTRODUCTION

A recent report describes the facility which has been developed at Argonne National Laboratory's FNG for (n,Xγ) reaction studies [1,2]. The geometry is shown in Figs.1-6 of Ref. 1 and it is recommended that the reader refer to this earlier report in conjunction with the present one.

Experience with this facility has indicated that the precision of raw data obtained generally improves with increased sample size. The relative importance of background decreases and the statistical accuracy of the significant data improves under these conditions. Furthermore, in measurements with relatively large samples, it is possible to exploit the advantages of longer flight paths (improved time-of-flight resolution) and massive detector shielding. The penalty involved in measurements with large samples is that corrections to the raw data for effects of absorption and multiple scattering can be quite large. Accurate determination of these corrections requires knowledge of neutron and photon cross sections and their angular distributions and use of complex computational procedures. Clearly, a compromise is necessary. The objective of this report is to present the results of a detailed study of sample-size effects which was conducted in the course of developing the data processing routines which are employed in the reduction of experimental data acquired with this facility.

The results of a literature survey were disappointing. There are relatively few readily available articles on the subject of sample corrections [3-13]. Most of these references deal with experiments in which neutrons (not gamma rays) are detected. These articles provided guidance, but were not a basis for the present work.

The analysis presented in this report employs only a few simplifying assumptions and therefore adheres to a

realistic representation of the physical problem.

The $^{7}Li(p,n)^{7}Be$ reaction is usually used as a neutron source at this laboratory for measurements in the region of interest for current $(n,X\gamma)$ studies ($E_n \lesssim 5$ MeV). Natural lithium metal is evaporated onto a thin tantalum backing to form a target. The proton-beam spot on target is defined by slits and is essentially rectangular. The lithium films are relatively thin ($\Delta E_p \lesssim 0.1$ MeV). The analysis presented in this report assumes an infinitesimally thin square target; however, the routines actually used for data processing take cognizance of realistic target thicknesses by superimposing contributions from several very thin layers. Target thickness is an important consideration whenever the cross section varies rapidly with neutron energy or for proton energies near the resonance in the lithium source reaction at $\sim$ 2.3 MeV. The angular distribution of neutrons from the source reaction is taken into account. Neutrons from the $^{7}Li(p,n)^{7}Be^{*}$ and $^{7}Li(p,n^{3}He)^{4}He$ reactions are considered in the analysis for proton energies above their production thresholds.

Gamma rays from $(n,X\gamma)$ reactions are detected with a Ge(Li) detector and the yields of full-energy-peak events are recorded. Since the Ge(Li) detector has a diameter of $\sim$ 5 cm and is placed $\sim$ 100-150 cm from the sample, it is assumed that the only photons which are capable of producing full-energy pulses in the detector are those which either experience no interaction in the sample after production via $(n,X\gamma)$ reactions or are coherently scattered in the sample. Therefore, the total photon cross section is assumed for sample absorption calculations and a small correction for coherent scattering is applied when necessary (see Appendix A).

The scattering of neutrons in the sample by elastic and inelastic scattering through discrete levels is treated.

The effects of more complicated reactions such as (n;2n), (n;n,p), (n;n,p), (n;n,α), etc. are insignificant for $E_n \lesssim 5$ MeV so they are ignored in the computations. Kinematic effects are considered, and energy-dependent cross sections and angular distributions are employed.

The scattering sample is assumed to be a uniform right-circular cylinder centered on the beam line with axis normal to the scattering plane defined by the beam line and the detector. Macroscopic cross sections are used in absorption calculations, and samples consisting of either single- or multiple-isotope elements, compounds or mixtures can be treated.

Let

Y_{TOT} = total observed gamma-ray yield for a particular geometry,

Y_0 = gamma-ray yield produced by unscattered neutrons,

Y_ℓ = gamma-ray yield produced by neutrons which have scattered "ℓ" times in the sample before initiating (n,Xγ) reactions,

k = highest order of scattering considered,

then

$$Y_{TOT} \lesssim Y_0 + \sum_{\ell=1}^{k} Y_\ell = Y_0 \left[1 + \sum_{\ell=1}^{k} (Y_\ell/Y_0)\right]. \qquad (1)$$

If

$$\alpha_\ell = (Y_\ell/Y_0), \qquad (2)$$

$$\alpha_{TOT} = \sum_{\ell=1}^{k} \alpha_\ell , \qquad (3)$$

then

$$Y_{TOT} \lesssim Y_0 (1 + \alpha_{TOT}). \qquad (4)$$

The symbol $\sum$ represents summation to avoid confusion with Σ used for macroscopic cross sections elsewhere in this report. The quantity α_{TOT} is called the multiple-

scattering parameter and α_ℓ is the ℓ-th component. For most samples,

$$\alpha_{TOT} < 1 \text{ and } \alpha_{\ell+1} << \alpha_\ell, \qquad (5)$$

and the sums in Eqs. 1 and 3 converge rapidly. Acceptable accuracy is obtained in practice for $k \leq 3$.

The evaluation of Y_0 and α_{TOT} are treated separately. The quantity Y_0 is determined analytically while α_{TOT} is deduced by Monte-Carlo methods.

The acquisition of nuclear data required for the computations is considered in Section 2; this is a problem which must be addressed before any sample-size correction factors can be computed. Section 3 of this report deals with evaluation of Y_0 and its relationship to the $(n,X\gamma)$ reaction differential cross section which is sought from the measurements. Section 4 treats the subject of multiple scattering and determination of α_{TOT}. In Section 5, the results of computations are compared with experimental data and a simplified computational procedure is explored.

2. NUCLEAR DATA FOR COMPUTATIONS

The methods for computation of sample correction factors described in this report are powerful in principle; however, the quality of the results obtained is only as good as the accuracy of the nuclear data utilized in the analysis. Thus, the experimenter must exercise judgement in selection of the sample size for an experiment. If the available cross section and angular distribution information is uncertain, it is necessary to use smaller samples and thereby sacrifice sensitivity and statistical accuracy in order to minimize the magnitude of the corrections which must be computed. Actually, the quality of available nuclear data is gradually improving, and high-

speed digital computers are accessible to most researchers. Therefore, it appears worthwhile to develop the sophisticated computational tools required to determine realistic corrections and exploit the experimental advantages of using relatively large samples whenever possible.

The existence of pronounced resonance structure in nuclear data complicates many aspects of nuclear science and technology; the present topic is no exception. It has been found convenient to smooth all energy-dependent nuclear data used in correction calculations with resolution functions which approximate the experimental conditions. The smoothed excitation functions can usually be represented with sufficient accuracy by a relatively small number of parameters. Fig. 1 demonstrates the concept. The use of smoothed cross sections for sample absorption and multiple-scattering calculations is an approximation, the validity of which must be investigated carefully prior to use in applications. One method is to compare the results of small- and large-sample measurements in regions where strong resonances are present in the cross sections.

Neutron cross section and angular distribution information is obtained from the evaluated neutron data file, ENDF/B-IV [14]; photon cross sections are obtained from an evaluation by Storm and Israel [15].

3. EFFECTS OF GEOMETRY AND ABSORPTION

The dominant features of the observed gamma-ray yield from (n,Xγ) reactions in the sample are determined by geometry and the absorption of neutron and gamma radiation. These features are predicted by the response of Y_0 in Eq. (4) to variation of the experimental conditions. Multiple scattering, represented by α_{TOT} in Eq.(4), yields a less significant correction to this behavior. This section describes the procedure used to compute Y_0 and presents the results of calculations designed to explore the sensitivity

of Y_0 to various parameters.

3.1 Mathematical Formalism

The yield for the entire sample is computed by summing the contributions from various portions of the sample. The neutron source and the sample are represented as described below. Fig. 2. illustrates the geometry.

Let

d_n = distance from a particular neutron source point to a particular sample point,

d_γ = distance from a particular sample point to the gamma-ray detector (assumed to be a single point),

δ_n = distance through the sample which the neutron must penetrate to reach the particular sample point,

δ_γ = distance through the sample which the gamma ray must penetrate to reach the gamma-ray detector,

R_S = radius of the sample,

H = height of the sample,

D_n = distance from the center of the neutron source to the center of the sample (which is also the pivot for the gamma-ray detector),

D_γ = distance from the center of the sample to the gamma-ray detector,

Θ_n = incident-neutron angle relative to the beam line,

Θ_{DET} = angle of gamma-ray detector relative to the beam line,

$\Theta_{n\gamma}$ = angle of emission of the gamma ray relative to the incident neutron,

F_n = absolute neutron-source strength of a uniform square source (neutrons/sr),

a = dimension of the square neutron source,

$(d\sigma/d\Omega)_\gamma$ = differential gamma-ray production cross section for the $(n,X\gamma)$ reaction,

(x_T,y_T,z_T) = coordinates for a point on the neutron-source surface,

(x_1,y_1,z_1) = coordinates for a point S_1 in the sample,

(x_D,y_D,z_D) = coordinates for the gamma-ray detector,

N_S = number of atoms per unit volume of the sample which can contribute to $(n,X\gamma)$ reactions,

Σ_{nT} = neutron macroscopic total cross section for the sample material,

$\Sigma_{\gamma T}$ = photon macroscopic total cross section for the sample material.

Two-body neutron-producing reactions are assumed in the present analysis. The neutron fluence F_n is a function of the reaction parameters, incident energy, and emission angle. Kinematics governs the variation of neutron energy with angle. The cross sections $(d\sigma/d\Omega)_\gamma$, Σ_{nT} and $\Sigma_{\gamma T}$ are energy-dependent; $(d\sigma/d\Omega)_\gamma$ also varies with angle $\Theta_{n\gamma}$.

The grid systems for the neutron source and the sample are illustrated in Fig. 2. The sample grid system used yields more uniformly sized elements than a standard cylindrical-coordinate grid system. The parameters which define these grid systems are

n_H = mesh for the sample height (the sample is divided into n_H layers of height H/n_H along the x-axis),

n_R = radial mesh (the sample is divided into a series of n_R-1 shells of thickness R_S/n_R plus a central cylinder with radius R_S/n_R),

n_ϕ = fundamental angular mesh (the central cylinder, j=1, is divided into n_ϕ wedges while

the jth shell has jn_ϕ segments, $j=2,\ldots,n_R$),

n_T = neutron-source mesh (the square source is divided into n_T^2 sections each with area a^2/n_T^2).

The total number of elements in the sample is $\frac{1}{2}n_H n_\phi n_R(n_R+1)$. The variation in volume of these elements depends only on the radial variable. Therefore

$$V_j = \frac{\pi R_S^2 H}{n_R^2 n_H n_\phi}\left(\frac{2j-1}{j}\right), \quad j=1,\ldots,n_R. \tag{6}$$

A constraint on the angular mesh n_ϕ, required for the type of sample grid used, is $n_\phi \geq 2$.

The intercept of the beam line and neutron source plane is selected as the origin of coordinates. The coordinates of the center of each neutron-source element are given by $(x_{T\alpha}, y_{T\beta}, z_T)$ where

$$x_{T\alpha} = \frac{a}{2n_T}(2\alpha - n_T - 1), \quad \alpha = 1,\ldots,n_T, \tag{7}$$

$$y_{T\beta} = \frac{a}{2n_T}(2\beta - n_T - 1), \quad \beta = 1,\ldots,n_T, \tag{8}$$

and $z_T = 0$ for all elements.

The coordinates of the gamma-ray detector are given by the formulas

$$y_D = D_\gamma \sin\theta_{DET}, \tag{9}$$

$$z_D = D_n + D_\gamma \cos\theta_{DET}, \tag{10}$$

and $x_D = 0$.

The coordinates of the center of each sample element are given by the formulas

$$x_{1i} = \frac{H}{2n_H}(2i - n_H - 1), \quad i=1,\ldots n_H, \tag{11}$$

$$y_{1jk} = r_j \sin\phi_{jk}, \quad j=1,\ldots,n_R \text{ and } k=1,\ldots,jn_\phi, \tag{12}$$

$$z_{ijk} = D_n + r_j \cos \phi_{jk},\ j=1,\ldots,n_R \text{ and } k=1,\ldots,jn_\phi, \tag{13}$$

and

$$r_j = \frac{R_S}{2n_R}(2j-1)\ ,\ j=1,\ldots,n_R\ , \tag{14}$$

$$\phi_{jk} = \frac{\pi}{jn_\phi}(2k-1)\ ,\ j=1,\ldots,n_R \text{ and } k=1,\ldots,jn_\phi \tag{15}$$

Analytic geometry is applied in derivation of formulas for δ_n and δ_γ. The expression for δ_n is

$$\delta_n = d_n - s_n\ , \tag{16}$$

where

$$d_n = [(x_1-x_T)^2 + (y_1 - y_T)^2 + (z_1 - z_T)^2]^{\frac{1}{2}}, \tag{17}$$

$$s_n = \frac{[B_n(y_0- y_T) + C_n(z_0- z_T)]}{(B_n^2 + C_n^2)} - \frac{\{(B_n^2 + C_n^2)R_S^2 - [C_n(y_T - y_0)-B_n(z_T- z_0)]^2\}^{\frac{1}{2}}}{(B_n^2 + C_n^2)}, \tag{18}$$

$$B_n = (y_1 - y_T)/d_n, \tag{19}$$

$$C_n = (z_1 - z_T)/d_n, \tag{20}$$

and (x_0,y_0,z_0) are the coordinates of the center of the sample ($x_0 = y_0 = 0$, $z_0 = D_n$). The expression for δ_γ is

$$\delta_\gamma = d_\gamma - s_\gamma\ , \tag{21}$$

where

$$d_\gamma = [(x_1- x_D)^2 + (y_1- y_0)^2 + (z_1- z_D)]^{\frac{1}{2}}\ , \tag{22}$$

$$s_\gamma = \frac{[B_\gamma(y_0- y_D) + C_\gamma(z_0- z_D)]}{(B_\gamma^2 + C_\gamma^2)} - \frac{\{(B_\gamma^2 + C_\gamma^2)R_S^2 - [C_\gamma(y_D- y_0)-B_\gamma(z_D- z_0)]^2\}^{\frac{1}{2}}}{(B_\gamma^2 + C_\gamma^2)}\ , \tag{23}$$

$$B_\gamma = (y_1- y_D)/d_\gamma\ , \tag{24}$$

$$C_\gamma = (z_1- z_D)/d_\gamma\ . \tag{25}$$

Let

η_n = neutron absorption factor,

η_γ = gamma-ray absorption factor,

then

$$\eta_n = \exp\left(-\Sigma_{nT}\delta_n\right) , \tag{26}$$

$$\eta_\gamma = \exp\left(-\Sigma_{\gamma T}\delta_\gamma\right) . \tag{27}$$

If

ε_{DET} = efficiency of the gamma-ray detector, defined as the ratio of detected (in the full-energy peak) to incident gamma rays,

then

$$Y_0 = \sum_{\alpha,\beta,i,j,k}^{n_T,n_H,n_R,n_\phi} \frac{F_n}{n_T^2}\left(\frac{\eta_n}{d_n^2}\right)\left(\frac{\eta_\gamma}{d_\gamma^2}\right) N_S (d\sigma/d\Omega)_\gamma V_j \varepsilon_{DET} . \tag{28}$$

Y_0 is a function of E_n and $\Theta_{n\gamma}$. The energy E_n lies in the range $(0,E_{n,max})$ while the scattering angle $\Theta_{n\gamma}$ is in the range $(0,\pi)$. Therefore, it is possible to define resolution functions $\mathscr{E}(E_n)$ and $\mathscr{A}(\Theta_{n\gamma})$ such that

$$Y_0 = \int_0^{E_{n,max}} \mathscr{E}(E_n)dE_n , \tag{29}$$

$$Y_0 = \int_0^{\pi} \mathscr{A}(\Theta_{n\gamma})d\Theta_{n\gamma} . \tag{30}$$

These resolution functions can be used to compute the average neutron energy $\langle E_n \rangle$ and the average scattering angle $\langle \Theta_{n\gamma} \rangle$ according to the formulas

$$\langle E_n \rangle = Y_0^{-1} \int_0^{E_{n,max}} E_n \, \mathscr{E}(E_n)dE_n , \tag{31}$$

$$\langle \Theta_{n\gamma} \rangle = Y_0^{-1} \int_0^{\pi} \Theta_{n\gamma} \, \mathscr{A}(\Theta_{n\gamma})d\Theta_{n\gamma} . \tag{32}$$

The relationship between Y_0 and the differential cross section $(d\sigma/d\Omega)_\gamma$ is indicated in Eq. (28). Let

$\langle (d\sigma/d\Omega)_\gamma \rangle$ = value of the differential cross section corresponding to neutron energy $\langle E_n \rangle$ and scattering angle $\langle \Theta_{n\gamma} \rangle$,

and define

$$\xi_\gamma = (d\sigma/d\Omega)_\gamma \; / \; \langle (d\sigma/d\Omega)_\gamma \rangle \; , \tag{33}$$

then Eq. (28) can be rewritten in the form

$$Y_0 = \langle (d\sigma/d\Omega)_\gamma \rangle \sum_{\alpha,\beta,i,j,k}^{n_T,n_H,n_R,n_\phi} \frac{F_n}{n_T^2} \left(\frac{\eta_n}{d_n^2}\right)\left(\frac{\eta_\gamma}{d_\gamma^2}\right) N_S \xi_\gamma V_j \epsilon_{DET} \tag{34}$$

which explicitly relates the gamma-ray yield to the differential cross section for a specific neutron energy and scattering angle. This formalism requires an approximate knowledge of ξ_γ (the shape of the differential cross section function in terms of neutron energy and scattering angle). In practice, most of the contributions to Y_0 come from limited ranges of neutron energy and scattering angle. Therefore, one estimates the behavior of ξ_γ for the regions of interest and applies this estimate in computations. Improved accuracy can be achieved by the process of iteration. Experience has shown no more than two passes are required for most applications.

3.2 Results of Numerical Studies

It is worthwhile to factor the gross solid-angle and sample-volume dependence from the expressions for Y_0. This can be achieved through definition of the quantity $\overline{Y}_0$ as follows:

$$Y_0 \equiv (\pi \, R_S^2 \, H \, D_n^{-2} D_\gamma^{-2}) \; \overline{Y}_0 \; . \tag{35}$$

In this section, sample geometry and absorption effects are investigated solely in terms of the behavior of $\overline{Y}_0$.

A Systems Engineering Laboratories Model 840 MP digital computer was utilized in computation of $\overline{Y}_0$ for various experimental conditions. A nominal parameter set for these calculations appears in Table I. The variation of $\overline{Y}_0$ in response to departures from the conditions represented by these parameters is investigated in the present section.

Selection of an appropriate set of mesh parameters n_T, n_H, n_R and n_ϕ is an important consideration. Coarse meshes lengthen the computation time unnecessarily. The computations were least sensitive to n_T and most sensitive to n_R as expected. The mesh parameters listed in Table I appear to be satisfactory for most practical applications.

The effects of radiation absorption were investigated by computing $\overline{Y}_0$ for four sets of parameters which differ from each other only in the assumed values for Σ_{nt} and $\Sigma_{\gamma T}$: i) neutron and gamma-ray absorption (Table I), ii) gamma-ray absorption only ($\Sigma_{nT} = 0$), iii) neutron absorption only ($\Sigma_{\gamma T} = 0$), and iv) no absorption ($\Sigma_{nT} = \Sigma_{\gamma T} = 0$). The effects of absorption are a reduction of gamma-ray yield and a distortion of the observed angular distribution. The relative gamma-ray yields at $\Theta_{\Delta ET} = 90°$ for these four cases are: i) 0.34, ii) 0.50, iii) 0.68, and iv) 1.00. The induced anisotropy for each situation is shown in Fig. 3. These distortions appear to be well represented by the expression

$$\overline{Y}_0 (\Theta_{DET}) \tilde{\approx} \overline{Y}_0 (90°) (1 - \Delta_0 \cos \Theta_{DET}) \qquad (36)$$

with Δ_0 assuming the following positive values for the four cases considered: i) 0.172, ii) 0.0658, iii) 0.0056,

and iv) 0.0021. Geometric effects and neutron attenuation alone produce very little distortion; however, gamma-ray absorption (particularly in combination with neutron absorption) skews the observed angular distribution about $\Theta_{DET} = 90°$ so that the back-angle yield exceeds the forward-angle yield.

The relative contributions to $\overline{Y}_0$ for $\Theta_{DET} = 90°$ from the midplane sample elements are presented for each of the four cases considered as follows: i) Fig. 4, ii) Fig. 5, iii) Fig. 6, and iv) Fig. 7. In conjunction with the results presented in Figs. 4-7, it is worthwhile to consider the ratios of yields from larger segments of the sample. Define the "back" of the sample as that half of the cylinder which is farthest from the neutron source, and the "front" of the sample as the opposite half. Similarly, label as "far" the sample half farthest from the gamma-ray detector. The opposite half is labelled as "near". Computed "front"-to-"back" and "near"-to-"far" ratios are listed in Table II.

The parameter D_n was varied over the range 5-50 cm with other parameters fixed at the values given in Table I. The value of $\overline{Y}_0$ for $\Theta_{DET} = 90°$ increased by only 3.3% as D_n increased from 5 to 50 cm. This would seem to imply that a parallel neutron beam approximation is warranted. However, variation in the distortion of the angular distribution was more pronounced as Δ_0 decreased from 0.268 for $D_n = 5$ cm to 0.121 for $D_n = 50$ cm. For small values of distance D_n, the sample subtends a sizeable solid angle so that the average scattering angle becomes quite sensitive to D_n. Therefore, use of the parallel neutron beam approximation is not recommended.

The parameter D_γ was varied over the range 30-200 cm with other parameters fixed at the values given in Table I. The value of $\overline{Y}_0$ for $\Theta_{DET} = 90°$ decreased by only 1.2%

as D_γ increased from 30 to 200 cm, and the distortion parameter Δ_0 decreased from 0.190 to 0.168. A parallel gamma ray approximation could be justified for these calculations.

Variation of the sample height H produces very little effect on $\overline{Y}_0$; however, the gamma-ray yield and distortion of the angular distribution depend critically upon the sample radius R_S. Computations were made for R_S = 0.635, 0.95, 1.27, 1.59, 1.905 and 2.54 cm with the other parameters fixed at the values listed in Table I. The results of these calculations appear in Table III. The near constancy of $R_S\ \overline{Y}_0$ for large values of R_S implies that, in this domain, the total gamma-ray yield from the sample increases more or less linearly with sample radius rather than as the square of the radius. The difference is due to absorption. Clearly, the total gamma ray yield from the sample also increases linearly with sample height. A set of calculations was made assuming no neutron or gamma-ray absorption and using values of H = 2 R_S ("square" samples). As R_S increases from 0.635 cm to 2.54 cm, $\overline{Y}_0$ decreases by 1.7%. This result indicates that the yield per unit volume depends only slightly on the size of the sample in the absence of absorption.

The most significant geometric effect is the loss of angular resolution which results from the use of large samples. The maximum geometric angular range for $\Theta_{n\gamma}$ associated with the conditions of Table I is $\sim 19°$. The contribution to this spread from the neutrons is $\sim 17°$ while that from the gamma rays is $\sim 2°$. The resolution functions $\mathscr{A}(\Theta_{n\gamma})$, as defined by Eq. (30), were determined for several values of Θ_{DET} using Table I parameters. The results are presented in Fig. 8. Values of $\langle\Theta_{n\gamma}\rangle$, computed with these resolution functions, differ significantly from the corresponding detector angles Θ_{DET} when Θ_{DET} approaches

0° or 180°. This result illustrates the well-known fact that relatively small samples are required for the measurement of differential cross sections near 0° or 180°.

Gamma-ray angular distributions for (n,Xγ) reactions are symmetric about $\Theta_{n\gamma} = 90°$. Computations were made using various assumed gamma-ray differential cross section functions $(d\sigma/d\Omega)_\gamma$. These calculations indicate that, for positive values of Δ_0, the formula

$$\overline{Y}_0 \approx (\text{Constant})\ (1 - \Delta_0 \cos \Theta_{DET}) \langle (d\sigma/d\Omega)_\gamma \rangle \qquad (37)$$

is valid to a considerable degree of accuracy. Furthermore, the distortion parameter Δ_0 and the average scattering angle $\langle \Theta_{n\gamma} \rangle$ are very insensitive to the shape of the differential cross section $(d\sigma/d\Omega)_\gamma$. Eq. (37) resembles Eq. (34) and it is concluded that the complicated sum given in Eq. (34) has a simple angular dependence. This particular result will be designated the "factorization rule" since it provides a prescription for relating the observed gamma-ray yield to the shape of the differential cross section. Fig. 9 demonstrates the factorization rule. This rule applies reasonably well for most realistic applications even when multiple scattering is taken into consideration (Section 4.2). Application of the factorization rule leads to a significant labor reduction in processing angular distribution data.

Realistically, the neutron field produced by proton bombardment of natural lithium is a mixture of first- and second-group neutrons plus some breakup neutrons at higher bombarding energies (Section 1). The energies and angular distributions of these components differ and this will influence the overall gamma-ray and monitor yields observed. Of concern, however, is the effect of superposition of contributions on the applicability of the factorization rule. To investigate this point, computations were made for several incident energies assuming realistic lithium first-

and second-group neutrons plus some breakup neutrons at higher bombarding energies (Section 1). The energies and angular distributions of these components differ and this will influence the overall gamma-ray and monitor yields observed. Of concern, however, is the effect of superposition of contributions on the applicability of the factorization rule. To investigate this point, computations were made for several incident energies assuming realistic lithium first- and second-group neutron sources as well as the hypothetical isotropic source identified in Table I. These calculations show that the distortion parameter Δ is relatively insensitive to the shape of the neutron-source reaction angular distribution. The parameter Δ varies with neutron energy since it depends on the total cross section. However, since $\Delta << 1$ for typical conditions, the energy dependence of Δ does not affect the angular distributions severely. For example, Δ is found to vary by $\sim$ 30% over the range E_n = 0.9-2 MeV for the sample described in Table I; however, the ratio $\overline{Y}_0(0°)/\overline{Y}_0(90°)$ varies by only $\sim$ 3% over this range. Therefore, it is often possible to apply the factorization rule for multigroup neutron sources. The formulas suggested by the results of numerical analysis are

$$\overline{Y}_0(\text{multigroup}) \tilde{\propto} (\text{Constant}) \; (1 - \langle \Delta \rangle \cos \Theta_{DET}) \; . \sum_m G_m \langle (d\sigma/d\Omega)_\gamma \rangle_m \; , \tag{38}$$

$$\langle \Delta \rangle = \left(\sum_m G_m \Delta_m \Big/ \sum_m G_m \right) \tag{39}$$

The parameters G_m depend upon the group intensities and sample absorption properties for neutrons in these groups.

The factorization rule is not a rigorous product of the formalism, but is an emperical concept which has been

distilled from the results of numerical calculations. Caution should be exercised when using this rule in processing data, particularly for measurements involving multigroup neutron sources.

4. EFFECTS OF NEUTRON MULTIPLE SCATTERING

The obvious result of multiple scattering is the enhancement of the observed yield relative to that predicted by the computations of the previous section. The objectives of the present section are to describe the method used for the evaluation of the multiple scattering parameter α_{TOT} and to investigate the dependence of multiple scattering on various experimental factors.

4.1 Mathematical Formalism

The approach taken in this work is to calculate values of Y_ℓ for $\ell = 0, 1, \ldots, k$ (see Section 1) by statistical methods and then compute the partial multiple-scattering parameters α_ℓ by means of Eq. (2). The total multiple-scattering parameter α_{TOT} is given by Eq. (3). There are several ways to formulate Monte-Carlo problems [13]. The present approach generally resembles that which is employed in multi-dimensional Monte-Carlo integration. The fundamental assumption of Monte-Carlo integration is that

$$\int_V d\vec{q}\, f(\vec{q}) \approx \frac{V}{N_{hist}} \sum_{i=1}^{N_{hist}} f(\vec{q}_i) \qquad (40)$$

for a sufficiently large number of histories N_{hist}, where $\vec{q}_i$ is selected at random from a region of ν-dimensional Cartesian space defined by

$$\vec{q} = (q_1, q_2, \ldots, q_\nu) \qquad (41)$$

$$d\vec{q} = (dq_1 dq_2 \ldots dq_\nu) \qquad (42)$$

$$V = (q_{1,max} - q_{1,min})\,(q_{2,max} - q_{2,min}) \ldots (q_{\nu,max} - q_{\nu,min}). \qquad (43)$$

The region of space defined by the volume V is a ν-dimensional rectangle and is selected so that the true region of interest lies entirely within V. The Monte-Carlo process consists of selecting points $\vec{q}_i$ at random in the larger region. If $\vec{q}_i$ falls outside the true region of interest, then $f(\vec{q}_i) = 0$ (a "miss"). This approach does not lead to optimum efficiency, however such wastefulness is usually tolerable with high-speed digital computers and avoids many computational complexities.

Some of the variables used in this analysis are defined in Sections 1 and 3; others are defined at appropriate points in the present section.

First, computation of Y_0 by Monte-Carlo methods is considered (see Fig. 10). The origin of coordinates is the neutron source (assumed here to be a point). The beam line is the z-axis, the sample axis is normal to the y - z plane as in Section 3. The center of the sample is at the coordinates $(0,0,D_n)$. The gamma-ray detector is a point in the y - z plane located a distance D_γ from the center of the sample. The first-scattering point S_1 in the sample is identified by the vector $\vec{x}_1$ with coordinates (x_1,y_1,z_1). A related spherical coordinate system can be defined by the equations

$$x_1 = r_1 \sin\theta_1 \cos\phi_1, \tag{44}$$

$$y_1 = r_1 \sin\theta_1 \sin\phi_1, \tag{45}$$

$$z_1 = r_1 \cos\theta_1. \tag{46}$$

The sample is located entirely within a region of space defined by the following expressions

$$r_{1,\min} \leq r_1 \leq r_{1,\max}, \tag{47}$$

$$r_{1,\min} = D_n - R_S, \tag{48}$$

$$r_{1,\max} = [(D_n + R_S)^2 + \tfrac{1}{4} H^2 + R_S^2]^{\frac{1}{2}}, \tag{49}$$

$$0 < \phi_1 < 2\pi, \tag{50}$$

$$0 \leq \theta_1 \leq \theta_{1,max}, \tag{51}$$

$$\theta_{1,max} = \tan^{-1}\left[(\tfrac{1}{4} H^2 + R_S^2)^{\frac{1}{2}}/(D_n - R_S)\right]. \tag{52}$$

The energy and angular dependence of all physical parameters is taken into consideration as well as kinematic effects. The gamma-ray yield from (n,Xγ) reactions initiated by unscattered neutrons is given by

$$Y_0 \approx \frac{V_1}{N_{hist}} \sum_{i=1}^{N_{hist}} \Gamma_{0i} \tag{53}$$

with

$$\Gamma_0 = \begin{cases} F_n \eta_1 \sin\theta_1 N_S (d\sigma/d\Omega)_\gamma \left(\frac{\eta_\gamma}{d_\gamma^2}\right) \epsilon_{DET} \\ \qquad \text{if } \vec{x}_1 \text{ is inside the sample,} \\ 0 \text{ otherwise (a "miss"),} \end{cases} \tag{54}$$

$$\eta_1 = \exp(-\delta_n \Sigma_{nT}) , \tag{55}$$

$$V_1 = 2\pi(r_{1,max} - r_{1,min})\theta_{1,max}. \tag{56}$$

For $\vec{x}_1$ to lie inside the sample, it is required that

$$-H/2 < x_1 < H/2 , \tag{57}$$

$$[y_1^2 + (z_1 - D_n)^2]^{\frac{1}{2}} < R_S . \tag{58}$$

Although determination of Y_0 by Monte-Carlo integration is technically simpler than the approach described in Section 3, it is slower since quite a few histories are required for convergence. Furthermore, it is not possible to derive the midplane-yield profile information presented in Figs. 4-7 from a simple Monte-Carlo treatment. However, for $\ell \geq 1$ it is impractical to determine Y_ℓ by any method other than Monte-Carlo analysis.

Next, consider computation of Y_1 (see Fig. 10). The scattering preceding the $(n,X\gamma)$ event can be either elastic or inelastic. The possibility for more than one neutron channel adds an additional complication to the computations. Some neutrons which scatter in the vicinity of point S_1 propagate toward point S_2 defined by the vector $\vec{x}_2$. Assume that there are N_1 distinct scattering processes applicable to the first scattering point S_1. The j-th process is defined by the parameters A_{1j}, Q_{1j} and $(d\Sigma/d\Omega)_{1j}$ where

A_{1j} = mass of the target nucleus,

Q_{1j} = reaction Q-value,

$(d\Sigma/d\Omega)_{1j}$ = macroscopic differential neutron-scattering cross section.

For simplicity, the inelastic scattering processes are assumed to be isotropic since they are nearly so in reality. Let ψ_1 be the total macroscopic scattering cross section defined by the equation

$$\psi_1 = \sum_{j=1}^{N_1} (d\Sigma/d\Omega)_{1j}, \tag{59}$$

then the relative probability P_{1j} of each process is given by the equation

$$P_{1j} = (d\Sigma/d\Omega)_{1j}/\psi_1. \tag{60}$$

Since

$$\sum_{j=1}^{N_1} P_{ij} = 1 , \tag{61}$$

the unit interval can be divided by a set of N_1 points $\{\rho_{1j}\}$ defined by the equation

$$\rho_{1j} = \sum_{\ell=1}^{j} P_{i\ell} . \tag{62}$$

A random number R is selected for each history. The neutron is then assumed to propagate from point S_1 to point S_2 by means of the j-th scattering process if

$$\rho_{1,j-1} < R \leq \rho_{1j} \quad . \tag{63}$$

Although the particular scattering process is selected by random sampling in the space of open channels, the macroscopic differential scattering cross section used in the computation is ψ_1.

A new spherical coordinate system with origin at S_1 is defined. The cartesian coordinates (origin at the neutron source) and spherical coordinates in the new system for point S_2 are related by the equations

$$x_2 = x_1 + r_2 \sin\Theta_2 \cos\phi_2 \quad , \tag{64}$$

$$y_2 = y_1 + r_2 \sin\Theta_2 \sin\phi_2 \quad , \tag{65}$$

$$z_2 = z_1 + r_2 \cos\Theta_2 . \tag{66}$$

The region of space defined by the expressions

$$0 \leq \Theta_2 \leq \pi \quad , \tag{67}$$

$$0 \leq \phi_2 \leq 2\pi \quad , \tag{68}$$

$$0 \leq r_2 \leq r_{2,max} \quad , \tag{69}$$

$$r_{2,max} = (H^2 + 8\,R_S^2)^{\frac{1}{2}} \quad , \tag{70}$$

encompasses the entire sample. Then,

$$Y_1 \approx \frac{V_1 V_2}{N_{hist}} \sum_{i=1}^{N_{hist}} \Gamma_{1i} \tag{71}$$

with

$$\Gamma_1 = \begin{cases} F_n\, \eta_1 \sin\Theta_1 \psi_1 \eta_2 \sin\Theta_2 \cdot \\ \quad \cdot N_S (d\sigma/d\Omega)_\gamma \left(\frac{\eta_\gamma}{d_\gamma^2}\right) \varepsilon_{DET} \\ \quad \text{if } \vec{x}_1 \text{ and } \vec{x}_2 \text{ are inside the sample,} \\ 0 \quad \text{otherwise (a "miss"),} \end{cases} \tag{72}$$

$$\eta_2 = \exp(-r_2 \Sigma_{nT}),$$

$$V_2 = 2\pi^2 r_{2,max}.$$

For $\vec{x}_2$ to lie inside the cylinder, it is required that

$$- H/2 < x_2 < H/2, \tag{73}$$

$$[y_2^2 + (z_2 - D_n)^2]^{\frac{1}{2}} < R_S \ . \tag{74}$$

Generalization to arbitrary orders of multiple scattering is straightforward. The expression for Y_k is

$$Y_k \overset{\sim}{\sim} \frac{V_1 V_2 \cdots V_{k+1}}{N_{hist}} \sum_{i=1}^{N_{hist}} \Gamma_{ki} \ , \tag{75}$$

with

$$\Gamma_k = \begin{cases} F_n\left(\pi_{\ell=1}^{k} \eta_\ell \sin\Theta_\ell \, \psi_\ell\right) \eta_{k+1} \sin\Theta_{k+1} \cdot \\ \quad \cdot N_S (d\sigma/d\Omega)_\gamma \left(\frac{\eta_\gamma}{d_\gamma^2}\right) \varepsilon_{DET} \\ \quad \text{if } \vec{x}_1 , \ldots , \vec{x}_{k+1} \text{ are inside the sample,} \\ 0 \quad \text{otherwise (a "miss").} \end{cases} \tag{76}$$

The parameters required for computation of all the higher-order scattering contributions resemble those described for computation of Y_1.

Values of $\Gamma_{0i}, \ldots , \Gamma_{ki}$ are computed for every history ($i=1, \ldots , N_{hist}$). Whenever a particular $\Gamma_{\ell i} = 0$ (a "miss"), the higher-order expressions $\Gamma_{\ell+1,i}, \ldots , \Gamma_{ki}$ are automatically equal to zero too. Thus, the efficiency for computation of Y_k declines with increased scattering order k. However,

$$Y_0 >> Y_1 >> .... >> Y_k \ , \tag{77}$$

so it is unnecessary to determine the high-order contributions to Y_{TOT} (Eq. 1) as accurately as the low-order contributions.

4.2 Results of Numerical Studies

Multiple-scattering calculations were performed with the SEL 840MP computer using a code named GAMSCT. This

code has been written in FORTRAN IV and a listing of the orders is given in Appendix B.

A nominal set of parameters, which provided a starting point for numerical studies of multiple scattering, is given in Table IV. Experience indicates that for k=3, satisfactory accuracy in computation of α_{TOT} is achieved for $N_{hist} \tilde{>} 100{,}000$. This value was selected for all calculations. Typical efficiencies ("hit" percentages) of the Monte-Carlo trials are as follows: Y_0(54.9%), Y_1(14.2%), Y_2(3.7%) and Y_3(0.8%). Relative values of Y_0, Y_1, Y_2 and Y_3 for various Θ_{DET} are plotted in Fig. 11. It is seen that the ratio $Y_{\ell+1}/Y_\ell$ is more or less independent of ℓ, and furthermore for all ℓ,

$$Y_\ell(\Theta_{DET}) \tilde{>} Y_\ell(90°)\ (1 - \Delta_\ell \cos \Theta_{DET}) , \qquad (78)$$

$$\Delta_0 > \Delta_1 > \Delta_2 > \Delta_3 \tilde{>} 0 . \qquad (79)$$

Intuitively, one expects the effects of geometric anisotropy to be washed out by multiple scattering. Eq. (79) supports this contention. Eq. (78) indicates that the factorization rule applies for an assumed isotropic differential cross section $(d\sigma/d\Omega)_\gamma$. Actually it also applies reasonably well for most realistic differential cross section functions. However, the factorization rule does fail in extreme cases where $(d\sigma/d\Omega)_\gamma$ approaches zero for $\Theta_{n\gamma} = 0°$ or 180°. Under these conditions, the observed yield for Θ_{DET} near 0° or 180° is dominated multiple scattering in a fashion which cannot be explained by a simple rule.

The effect of sample size was tested by varying R_S and H ($H = 2R_S$) with respect to the values in Table IV. The results are presented in Fig. 12. The contributions from second- and higher-order scattering are negligible for small samples. Variation of D_n and D_γ over realistic ranges produced very little effect on the computed multiple-scattering parameters.

Computations performed with various assumed realistic neutron-source reactions indicate that the multiple-scattering correction parameters are relatively insensitive to the properties of the neutron source. Therefore, it is reasonable to compute α_{TOT} for various energies E_n and angles Θ_{DET} assuming an isotropic, monoenergetic neutron source.

The multiple-scattering parameters are relatively insensitive to Σ_{nT} and $\Sigma_{\gamma T}$. However, they depend critically on the magnitudes of the scattering cross sections. The relationship

$$\alpha_\ell \approx (\text{Constant})\Sigma_{EL}^{\ell} \tag{80}$$

gives a rough indication of this dependence for the simple case of energy-independent elastic scattering. The multiple scattering parameters are considerably less sensitive to the shape of the neutron scattering angular distributions.

5. COMPARISON OF EXPERIMENTAL AND COMPUTED RESULTS FOR NATURAL IRON SAMPLES

Measurements were performed with seven natural iron samples to test the validity of the methods described in this report. The sizes of the samples investigated were R_S = 0.635, 0.953, 1.27, 1.59, 1.91, 2.22 and 2.54 cm ($H = 2\ R_S$). Realistic energy-averaged cross sections were utilized in the computations (Section 2 and Refs. 14 and 15). The facility described in Ref. 1 was utilized for the irradiations. A 0.1-MeV-thick natural lithium target was bombarded with 3.68-MeV protons. Approximately 90% of the neutrons originated from the $^7Li(p,n)^7Be$ reaction ($E_n \approx 2$ MeV) and 10% came from the $^7Li(p,n)^7Be^*$ reaction ($E_n \approx 1.535$ MeV); the proton energy was slightly

below threshold for the $^{7}Li(p,n^{3}He)^{4}He$ breakup reaction. The Ge(Li) detector was situated at $\Theta_{DET} = 90°$. The relative neutron fluence was monitored by time-of-flight techniques using a plastic scintillator.

The full-energy peak yields for the 0.846-MeV line from the $^{56}Fe(n,n'\gamma)^{56}Fe$ reaction were divided by the masses of the corresponding samples (proportional to the volume) to determine quantities proportional to the yield per atom. All measurements were performed in identical geometry, so the yields per atom deduced are proportional to $\bar{Y}_0 (1 + \alpha_{TOT})$ as defined in Sections 1-4.

Measurements for samples with $R_S < 0.635$ cm were not practical because of background problems; however, computations were performed for a wide range of sample sizes including R_S near zero. In the limit of very small samples, geometry, absorption and multiple-scattering effects vanish. The experimental and computed values were normalized so that the yield per atom approaches unity for very small samples.

Four sets of computations were performed. The assumptions made in these calculations are as follows: i) no absorption, geometric corrections only, ii) absorption of neutrons and gamma-rays with the neutron total cross section used for absorption calculations and multiple scattering neglected, iii) identical to (ii) except that the total non-elastic cross section is used for the neutron absorption calculations, and iv) identical to (ii) except multiple scattering is considered (most realistic approach). The results of these calculations are compared with the experimental data in Fig. 13. The calculations labelled (iii) and (iv) both agree well with the experimental results; the agreement of set (iv) values is superior as anticipated. The agreement for such a wide range of sample sizes is very encouraging

(the diameter of the largest sample considered is equivalent to 1.4 mean free path lengths for neutrons and 2.5 mean free path lengths for 0.846-MeV photons).

The assumptions made for the set (iii) calculations were suggested by Day [3]. The Day approximation is widely used by researchers in the analysis of (n,Xγ) data. It is appealing because it eliminates the necessity for performing multiple-scattering calculations. The results shown in Fig. 13 correspond to $\theta_{DET} = 90°$. Computations were performed to compare the predictions of the Day approximation with those from the more realistic treatment at other angles. The results of this analysis show that these two approaches yield results which agree within ∿ 3% for $\theta_{DET} = 90° - 150°$; however, the agreement for $\theta_{DET} = 30° - 90°$ is only within ∿ 7% (for an iron sample with $R_S = 1.9$ cm). This suggests that for careful work, where accuracies of better than 10% are sought, it is advisable to employ a realistic treatment which includes multiple-scattering analysis. In applications where such accuracy is not sought, or is unfeasible, the Day approximation appears to be warranted since it saves considerable labor.

6. CONCLUSIONS

The formalism described in this report provides a means for determining differential cross section data for (n,Xγ) reactions from measurements made using relatively large cylindrical samples provided that accurate absorption and scattering cross section data is available.

Geometric effects reduce angular resolution and make it difficult to measure differential cross sections near 0° or 180°; otherwise, they have a relatively minor influence on the measurements.

The absorption of radiation reduces the overall yield and distorts angular distributions. Under most conditions, this distortion assumes the form $1-\Delta \cos\theta_{DET}$

($\Delta>0$); the shape of the differential cross section can be deduced from the experimental data by factoring out this simple angular dependence. Factorization is possible, even in the presence of multiple scattering, for most realistic situations and this saves considerable labor in processing data.

The Day approximation [3] permits one to avoid making detailed multiple scattering calculations, and appears to be an acceptable approach when accuracies of no better than $\sim$ 10% are acceptable.

ACKNOWLEDGEMENTS

The author is indebted to J. W. Meadows and P. T. Guenther for valuable suggestions offered during the course of this work.

APPENDIX A

COHERENT PHOTON SCATTERING

Photons which scatter coherently in the sample are indistinguishable from those which suffer no interaction. The coherent scattering cross sections depend upon photon energy E_γ and atomic number Z. They decrease rapidly with E_γ. For this reason, the coherent scattering corrections are relatively small for most materials of interest when E_γ exceeds a few hundred kilovolts.

In order to estimate the correction, a model which assumes a well-defined, distributed gamma-ray source intensity in a solid cylinder is employed. The unscattered and coherently-scattered photon yield at a distant detector is computed as described below.

If $\Sigma_{\gamma,COH}$ is the integrated macroscopic coherent scattering cross section, then the macroscopic differential scattering cross section is given by

$$(d\Sigma/d\Omega)_{\gamma,COH} = \frac{3\Sigma_{\gamma,COH}}{16\pi} (1 + \cos^2 \Theta_\gamma) . \qquad (81)$$

Assume that the cylinder is divided into a large number of discrete elements. Let

$\vec{x}_i$ = coordinates of the center of the i-th element

ΔV_i = isotropic gamma-ray source strength density for the ith component (gamma rays/sr/cm^3),

$\vec{x}_\Delta$ = coordinates of the detector.

δ_i = distance through sample material which the photon must penetrate to reach the detector if it originates at point $\vec{x}_i$. (See Section 3),

Y_U = yield at the detector due to unscattered photons

Y_S = yield due to photons which have scattered once coherently in the sample.

$$Y_U \approx \sum_i \frac{S_i \Delta V_i \exp(-\Sigma_{\gamma T}\delta_i)}{|\vec{x}_{Oi} - \vec{x}_D|} \varepsilon_{DET} , \qquad (82)$$

$$Y_S \approx \sum_{ij} \frac{S_i \Delta V_i \Delta V_j \exp[-\Sigma_{\gamma T}(\delta_i + |\vec{x}_i - \vec{x}_j|)]}{|\vec{x}_i - \vec{x}_j|^2 |\vec{x}_j - \vec{x}_D|^2} \cdot$$

$$\cdot (d\Sigma/d\Omega)_{\gamma,COH,ij} \varepsilon_{DET} \qquad (83)$$

The problem has been formulated in cylindrical coordinates and a code is available for operation on the SEL 840 MP digital computer. A number of calculations were performed assuming a constant value for S_i throughout the sample. Samples with R_S = 1.9 cm and H = 3.8 cm, fabricated from Li, Aℓ, Ti, Fe, Zn and Mo, were considered. The detector was assumed to be 130 cm from the sample. The ratio $Y_U/(Y_U+Y_S)$ was computed for E_γ = 0.1, 0.3, 0.5, 0.8, 1.0, 2.0 and 5.0 for these samples. The results appear in Table V. The coherent scattering correction is clearly quite small if not negligible for most cases of interest.

APPENDIX B

LISTING OF CODE GAMSCT

Code GAMSCT was developed to perform the multiple-scattering computations discussed in Section 4 of this report. This code is written in ASI Standard FORTRAN IV. All code input is from cards (Unit 4). Output is produced on a teletype (Unit 1) and a line printer (Unit 5). The version of this code listed here is operated on a Systems Engineering Laboratories Model 840 MP digital computer.

```
C      GAMSCT-D.L.SMITH-SEL 840MP                                                GMSCT   1
C                                                                                GMSCT   2
       DIMENSIØN ENT(25),SIGNT(25),EGP(25),SIGGP(25),NWGP(6),EWGP(6,15),WGMSCT   3
      1GP(6,15),QNS(6),A2NS(6),NNS(6),ENS(6,25),SIGNS(6,25),MWNS(6),NWNS(GMSCT   4
      26,10),EWNS(6,10,15),WNS(6,10,15),DSIGNS(6),WT(10),YLD(5),YLDSUM(5)GMSCT   5
      3,PSI(6),INDEX(4),JNDEX(5),NHIT(5),NLEV(6),A(25),B(25),WØRK(25)     GMSCT   6
C                                                                                GMSCT   7
       DATA PI/3.14159/                                                          GMSCT   8
C                                                                                GMSCT   9
       VALUE(V,VMIN,VMAX)=VMIN+V*(VMAX-VMIN)                                     GMSCT  10
       SEPAR(X1,Y1,Z1,X2,Y2,Z2)=SQRT((X1-X2)*(X1-X2)+(Y1-Y2)*(Y1-Y2)+(Z1-GMSCT  11
      1Z2)*(Z1-Z2))                                                              GMSCT  12
C                                                                                GMSCT  13
C      CØNTRØL                                                                   GMSCT  14
C                                                                                GMSCT  15
    1  READ(4,2) IC                                                             GMSCT  16
    2  FØRMAT(I1)                                                               GMSCT  17
       GØ TØ(10,20,30,50),IC                                                    GMSCT  18
   10  PAUSE                                                                    GMSCT  19
       GØ TØ 1                                                                  GMSCT  20
C                                                                               GMSCT  21
C      READ INTERPØLATIØN TABLES                                                GMSCT  22
C                                                                               GMSCT  23
   20  READ(4,21) MNT                                                           GMSCT  24
   21  FØRMAT(16I5)                                                             GMSCT  25
       READ(4,22) (ENT(I),SIGNT(I),I=1,MNT)                                     GMSCT  26
   22  FØRMAT(8E10.4)                                                           GMSCT  27
       READ(4,21) MGP                                                           GMSCT  28
       READ(4,22) (EGP(I),SIGGP(I),I=1,MGP)                                     GMSCT  29
       READ(4,21) MWGP                                                          GMSCT  30
       IF(MWGP) 23,25,23                                                        GMSCT  31
   23  DØ 24 I=1,MWGP                                                           GMSCT  32
       READ(4,21) NWGP(I)                                                       GMSCT  33
       M=NWGP(I)                                                                GMSCT  34
   24  READ(4,22) (EWGP(I,J),WGP(I,J),J=1,M)                                    GMSCT  35
   25  READ(4,21) MNS                                                           GMSCT  36
       DØ 28 I=1,MNS                                                            GMSCT  37
       READ(4,22) QNS(I),A2NS(I)                                                GMSCT  38
       READ(4,21) NNS(I)                                                        GMSCT  39
       M=NNS(I)                                                                 GMSCT  40
       READ(4,22) (ENS(I,J),SIGNS(I,J),J=1,M)                                   GMSCT  41
       READ(4,21) MWNS(I)                                                       GMSCT  42
       IF(MWNS(I)) 26,28,26                                                     GMSCT  43
   26  L=MWNS(I)                                                                GMSCT  44
       DØ 27 J=1,L                                                              GMSCT  45
       READ(4,21) NWNS(I,J)                                                     GMSCT  46
       M=NWNS(I,J)                                                              GMSCT  47
   27  READ(4,22) (EWNS(I,J,K),WNS(I,J,K),K=1,M)                                GMSCT  48
   28  CØNTINUE                                                                 GMSCT  49
C                                                                               GMSCT  50
C      READ AND WRITE BASIC PARAMETERS                                          GMSCT  51
C                                                                               GMSCT  52
   30  READ(4,31) NSCAT,NHIST                                                   GMSCT  53
   31  FØRMAT(I1,I6)                                                            GMSCT  54
       READ(4,22) RS,H,DN0,DG0                                                  GMSCT  55
       READ(4,22) EG,SIGGT,ENTHG                                                GMSCT  56
       READ(4,22) A1T,A2T,QT                                                    GMSCT  57
       READ(4,32) ET,NWT                                                        GMSCT  58
   32  FØRMAT(E10.4,I5)                                                         GMSCT  59
```

```
      IF(NWT) 34,34,33
   33 READ(4,22) (WT(I),I=1,NWT)
   34 WRITE(5,35) NSCAT,NHIST
   35 FORMAT(1H1/11HNSCAT,NHIST/I1,I6)
      WRITE(5,36) RS,H,DN0,DG0
   36 FORMAT(12HRS,H,DN0,DG0/4E10.4)
      WRITE(5,37) EG,SIGGT,ENTHG
   37 FORMAT(14HEG,SIGGT,ENTHG/3E10.4)
      WRITE(5,38) A1T,A2T,QT
   38 FORMAT(10HA1T,A2T,QT/3E10.4)
      WRITE(5,39) ET,NWT
   39 FORMAT(6HET,NWT/E10.4,I5)
      IF(NWT) 40,42,40
   40 WRITE(5,41)
   41 FORMAT(5HWT(I))
      WRITE(5,22) (WT(I),I=1,NWT)
   42 WRITE(5,43)
   43 FORMAT(/5H.....)
C
C     READ AND WRITE SCATTERING ANGLE, CONVERT TO RADIANS
C
   50 READ(4,22) THTANK
      WRITE(5,51) THTANK
   51 FORMAT(/7HTHTANK=,E10.4)
      THDET=PI*THTANK/180.0
C
C     PRELIMINARY CALCULATIONS
C
      RSRS=RS*RS
      HH=H*H
      HD2=0.5*H
      R1MIN=DN0-RS
      R1MAX=SQRT(DN0*DN0+2.0*DN0*RS+2.0*RSRS+0.25*HH)
      TH1MAX=ATAN(SQRT(0.25*HH+RSRS)/R1MIN)
      VOL1=2.0*PI*(R1MAX-R1MIN)*TH1MAX
      RMAX=SQRT(HH+8.0*RSRS)
      VOLH=2.0*PI*PI*RMAX
      YD=DG0*SIN(THDET)
      ZD=DN0+DG0*COS(THDET)
      DO 60 I=1,NSCAT
      NHIT(I)=0
   60 YLDSUM(I)=0.0
      DO 61 I=1,MNS
   61 NLEV(I)=0
      IHIST=1
C
C.....START OF HISTORY LOOP
C
C
  100 DO 101 I=1,NSCAT
  101 JNDEX(I)=0
C
C     SELECT SCATTERING POINT S(1)
C
      R=RANF(-1)
      RR=VALUE(R,R1MIN,R1MAX)
      R=RANF(-1)
      TH=VALUE(R,0.0,TH1MAX)
      R=RANF(-1)
      PHI=VALUE(R,0.0,2.0*PI)
```

GMSCT 60 GMSCT 61 GMSCT 62 GMSCT 63 GMSCT 64 GMSCT 65 GMSCT 66 GMSCT 67 GMSCT 68 GMSCT 69 GMSCT 70 GMSCT 71 GMSCT 72 GMSCT 73 GMSCT 74 GMSCT 75 GMSCT 76 GMSCT 77 GMSCT 78 GMSCT 79 GMSCT 80 GMSCT 81 GMSCT 82 GMSCT 83 GMSCT 84 GMSCT 85 GMSCT 86 GMSCT 87 GMSCT 88 GMSCT 89 GMSCT 90 GMSCT 91 GMSCT 92 GMSCT 93 GMSCT 94 GMSCT 95 GMSCT 96 GMSCT 97 GMSCT 98 GMSCT 99 GMSCT100 GMSCT101 GMSCT102 GMSCT103 GMSCT104 GMSCT105 GMSCT106 GMSCT107 GMSCT108 GMSCT109 GMSCT110 GMSCT111 GMSCT112 GMSCT113 GMSCT114 GMSCT115 GMSCT116 GMSCT117 GMSCT118 GMSCT119

```
      SINTH=SIN(TH)                                                      GMSCT120
      X=RR*SINTH*COS(PHI)                                                GMSCT121
      Y=RR*SINTH*SIN(PHI)                                                GMSCT122
      Z=RR*COS(TH)                                                       GMSCT123
      IF(X+HD2) 700,700,150                                              GMSCT124
  150 IF(X-HD2) 151,700,700                                              GMSCT125
  151 ZMDNO=Z-DNO                                                        GMSCT126
      TEST=Y*Y+ZMDNO*ZMDNO                                               GMSCT127
      IF(TEST-RSRS) 152,700,700                                          GMSCT128
  152 JNDEX(1)=1                                                         GMSCT129
      NHIT(1)=NHIT(1)+1                                                  GMSCT130
      CALL ANGLE(X,Y,Z,0.0,0.0,0.0,0.0,0.0,0.0,0.0,0.0,0.0,DNO,0.0,0.0,0.0,0.0,0.0,THT)  GMSCT131
C                                                                        GMSCT132
C     CALCULATE NEUTRON ENERGY AND FLUX AT POINT S(1)                    GMSCT133
C                                                                        GMSCT134
      CALL KINAM(A1T,A2T,1.00867,QT,ET,THT,EN,EDUM)                      GMSCT135
      IF(EN-ENTHG) 700,700,160                                           GMSCT136
  160 CALL DISTR(WT,THT,FT,NWT,10)                                       GMSCT137
      DELTN=DELTA(0.0,0.0,DNO,0.0,0.0,0.0,0.0,X,Y,Z,RS,1)                GMSCT138
      CALL INTRPL(MNT,ENT,SIGNT,EN,VSNT)                                 GMSCT139
      ETAN=EXF(-VSNT*DELTN)                                              GMSCT140
      FLUX=FT*ETAN*SIN(TH)*VOL1                                          GMSCT141
C                                                                        GMSCT142
C     CALCULATE GAMMA PRODUCTION FROM POINT S(1)                         GMSCT143
C                                                                        GMSCT144
      DG=SEPAR(X,Y,Z,0.0,YD,ZD)                                          GMSCT145
      CALL INTRPL(MGP,EGP,SIGGP,EN,VSGP)                                 GMSCT146
      IF(MWGP) 170,170,200                                               GMSCT147
  170 DSIGGP=VSGP/4.0/PI                                                 GMSCT148
      GO TO 203                                                          GMSCT149
  200 DO 202 I=1,MWGP                                                    GMSCT150
      M=NWGP(I)                                                          GMSCT151
      DO 201 J=1,M                                                       GMSCT152
      A(J)=EWGP(I,J)                                                     GMSCT153
  201 B(J)=WGP(I,J)                                                      GMSCT154
  202 CALL INTRPL(M,A,B,EN,WORK(I))                                      GMSCT155
      CALL ANGLE(0.0,YD,ZD,X,Y,Z,X,Y,Z,0.0,0.0,0.0,0.0,0.0,THNG)        GMSCT156
      CALL DISTR(WORK,THNG,SG,MWGP,10)                                   GMSCT157
      DSIGGP=VSGP*SG/4.0/PI                                              GMSCT158
  203 DELTG=DELTA(0.0,0.0,DNO,0.0,YD,ZD,X,Y,Z,RS,1)                      GMSCT159
      ETAG=EXF(-SIGGT*DELTG)                                             GMSCT160
      YLDG=FLUX*DSIGGP*ETAG/DG/DG                                        GMSCT161
C                                                                        GMSCT162
C     UPDATE YLDSUM(1)                                                   GMSCT163
C                                                                        GMSCT164
      YLDSUM(1)=YLDSUM(1)+YLDG                                           GMSCT165
C                                                                        GMSCT166
C     CHECK IF MULTIPLE SCATTERING CALCULATIONS ARE REQUESTED.           GMSCT167
C     INITIALIZE PARAMETERS IF REQUIRED                                  GMSCT168
C                                                                        GMSCT169
      IF(NSCAT-1) 240,700,240                                            GMSCT170
  240 ISCAT=2                                                            GMSCT171
      XSAV1=0.0                                                          GMSCT172
      YSAV1=0.0                                                          GMSCT173
      ZSAV1=0.0                                                          GMSCT174
      XSAV2=X                                                            GMSCT175
      YSAV2=Y                                                            GMSCT176
      ZSAV2=Z                                                            GMSCT177
      DO 250 I=2,NSCAT                                                   GMSCT178
      J=I-1                                                              GMSCT179
```

```
  250 INDEX(J)=0                                                                GMSCT180
C                                                                               GMSCT181
CXXX  START ØF MULTIPLE SCATTERING LØØP                                         GMSCT182
C                                                                               GMSCT183
C     SELECT SCATTERING PØINT S(ISCAT)                                          GMSCT184
C                                                                               GMSCT185
  300 R=RANF(-1)                                                                GMSCT186
      RR=VALUE(R,0.0,RMAX)                                                      GMSCT187
      R=RANF(-1)                                                                GMSCT188
      TH=VALUE(R,0.0,PI)                                                        GMSCT189
      R=RANF(-1)                                                                GMSCT190
      PHI=VALUE(R,0.0,2.0*PI)                                                   GMSCT191
      SINTH=SIN(TH)                                                             GMSCT192
      X=XSAV2+RR*SINTH*CØS(PHI)                                                 GMSCT193
      Y=YSAV2+RR*SINTH*SIN(PHI)                                                 GMSCT194
      Z=ZSAV2+RR*CØS(TH)                                                        GMSCT195
      IF(X+HD2) 700,700,350                                                     GMSCT196
  350 IF(X-HD2) 351,700,700                                                     GMSCT197
  351 ZMDN0=Z-DN0                                                               GMSCT198
      TEST=Y*Y+ZMDN0*ZMDN0                                                      GMSCT199
      IF(TEST-RSRS) 352,700,700                                                 GMSCT200
  352 JNDEX(ISCAT)=1                                                            GMSCT201
      NHIT(ISCAT)=NHIT(ISCAT)+1                                                 GMSCT202
      CALL ANGLE(X,Y,Z,XSAV2,YSAV2,ZSAV2,XSAV2,YSAV2,ZSAV2,XSAV1,YSAV1,ZGMSCT203
     1SAV1,THSCT)                                                               GMSCT204
C                                                                               GMSCT205
C     SELECT NEUTRØN SCATTERING PRØCESS FØR PØINT S(ISCAT-1)                    GMSCT206
C                                                                               GMSCT207
      DØ 407 I=1,MNS                                                            GMSCT208
      EB=-QNS(I)*(1.0+(1.0087/(A2NS(I)-1.0087))-(0.5*QNS(I)/(A2NS(I)-1.0GMSCT209
     1087)/931.478))                                                            GMSCT210
      IF(EN-EB) 400,400,401                                                     GMSCT211
  400 DSIGNS(I)=0.0                                                             GMSCT212
      GØ TØ 407                                                                 GMSCT213
  401 M=MNS(I)                                                                  GMSCT214
      DØ 402 J=1,M                                                              GMSCT215
      A(J)=ENS(I,J)                                                             GMSCT216
  402 B(J)=SIGNS(I,J)                                                           GMSCT217
      CALL INTRPL(M,A,B,EN,VSSCT)                                               GMSCT218
      IF(MWNS(I)) 403,403,404                                                   GMSCT219
  403 DSIGNS(I)=VSSCT/4.0/PI                                                    GMSCT220
      GØ TØ 407                                                                 GMSCT221
  404 M=MWNS(I)                                                                 GMSCT222
      DØ 406 J=1,M                                                              GMSCT223
      L=NWNS(I,J)                                                               GMSCT224
      DØ 405 K=1,L                                                              GMSCT225
      A(K)=EWNS(I,J,K)                                                          GMSCT226
  405 B(K)=WNS(I,J,K)                                                           GMSCT227
  406 CALL INTRPL(L,A,B,EN,WØRK(J))                                             GMSCT228
      CALL DISTR(WØRK,THSCT,SSCT,M,10)                                          GMSCT229
      DSIGNS(I)=VSSCT*SSCT/4.0/PI                                               GMSCT230
  407 CØNTINUE                                                                  GMSCT231
      SUMSCT=0.0                                                                GMSCT232
      DØ 408 I=1,MNS                                                            GMSCT233
  408 SUMSCT=SUMSCT+DSIGNS(I)                                                   GMSCT234
      IF(SUMSCT) 409,700,409                                                    GMSCT235
  409 PSI(1)=0.0                                                                GMSCT236
      K=MNS+1                                                                   GMSCT237
      PSI(K)=1.0                                                                GMSCT238
      IF(MNS-1) 410,410,411                                                     GMSCT239
```

```
  410 INDX=1                                                          GMSCT240
      GØ TØ 414                                                       GMSCT241
  411 SUMPSI=0.0                                                      GMSCT242
      DØ 413 I=2,MNS                                                  GMSCT243
      J=I-1                                                           GMSCT244
      SUMPSI=SUMPSI+DSIGNS(J)                                         GMSCT245
      PSI(I)=SUMPSI/SUMSCT                                            GMSCT246
      IF(PSI(I)-1.0) 413,413,412                                      GMSCT247
  412 PSI(I)=1.0                                                      GMSCT248
  413 CØNTINUE                                                        GMSCT249
      R=RANF(-1)                                                      GMSCT250
      CALL FINDI(PSI,K,6,R,INDX)                                      GMSCT251
  414 NLEV(INDX)=NLEV(INDX)+1                                         GMSCT252
C                                                                     GMSCT253
C     CALCULATE NEUTRØN ENERGY AND FLUX AT PØINT S(ISCAT)             GMSCT254
C                                                                     GMSCT255
  500 ENSAV=EN                                                        GMSCT256
      CALL KINAM(1.0087,A2NS(INDX),1.0087,QNS(INDX),ENSAV,THSCT,EN,FDUM)GMSCT257
      IF(EN-ENTHG) 700,700,501                                        GMSCT258
  501 CALL INTRPL(MNT,ENT,SIGNT,EN,VSNT)                              GMSCT259
      ETAN=EXF(-VSNT*RR)                                              GMSCT260
      FLUX=FLUX*SUMSCT*ETAN*SIN(TH)*VØLH                              GMSCT261
C                                                                     GMSCT262
C     CALCULATE GAMMA PRØDUCTIØN FRØM PØINT S(ISCAT)                  GMSCT263
C                                                                     GMSCT264
      DG=SEPAR(X,Y,Z,0.0,YD,ZD)                                       GMSCT265
      CALL INTRPL(MGP,EGP,SIGGP,EN,VSGP)                              GMSCT266
      IF(MWGP) 502,502,600                                            GMSCT267
  502 DSIGGP=VSGP/4.0/PI                                              GMSCT268
      GØ TØ 603                                                       GMSCT269
  600 DØ 602 I=1,MWGP                                                 GMSCT270
      M=NWGP(I)                                                       GMSCT271
      DØ 601 J=1,M                                                    GMSCT272
      A(J)=EWGP(I,J)                                                  GMSCT273
  601 B(J)=WGP(I,J)                                                   GMSCT274
  602 CALL INTRPL(M,A,B,EN,WØRK(I))                                   GMSCT275
      CALL ANGLE(0.0,YD,ZD,X,Y,Z,X,Y,Z,XSAV2,YSAV2,ZSAV2,THNG)        GMSCT276
      CALL DISTR(WØRK,THNG,SG,MWGP,10)                                GMSCT277
      DSIGGP=VSGP*SG/4.0/PI                                           GMSCT278
  603 DELTG=DELTA(0.0,0.0,DN0,0.0,YD,ZD,X,Y,Z,RS,1)                   GMSCT279
      ETAG=EXF(-SIGGT*DELTG)                                          GMSCT280
      YLDG=FLUX*DSIGGP*ETAG/DG/DG                                     GMSCT281
C                                                                     GMSCT282
C     UPDATE YLDSUM(ISCAT) AND FIX INDEX(ISCAT-1)                     GMSCT283
C                                                                     GMSCT284
      YLDSUM(ISCAT)=YLDSUM(ISCAT)+YLDG                                GMSCT285
      J=ISCAT-1                                                       GMSCT286
      INDEX(J)=INDX                                                   GMSCT287
C                                                                     GMSCT288
C     TEST FØR END ØF MULTIPLE SCATTERING LØØP, RESET PARAMETERS FØR  GMSCT289
C     NEXT CYCLE IF REQUIRED                                          GMSCT290
C                                                                     GMSCT291
      ISCAT=ISCAT+1                                                   GMSCT292
      IF(ISCAT-NSCAT) 610,610,700                                     GMSCT293
  610 XSAV1=XSAV2                                                     GMSCT294
      YSAV1=YSAV2                                                     GMSCT295
      ZSAV1=ZSAV2                                                     GMSCT296
      XSAV2=X                                                         GMSCT297
      YSAV2=Y                                                         GMSCT298
      ZSAV2=Z                                                         GMSCT299
```

```
      GØ TØ 300
C                                                                       GMSCT300
CXXX  END ØF MULTIPLE SCATTERING LØØP                                   GMSCT301
C                                                                       GMSCT302
C     UPDATE HISTØRIES AVERAGE, INTERMEDIATE ØUTPUT IF SS1 UP, TEST     GMSCT303
C     FØR CØMPLETIØN ØF REQUESTED NUMBER ØF HISTØRIES ØR SS2 UP AND     GMSCT304
C     PRØCEED TØ ØUTPUT ØR CØNTINUE WITH HISTØRY ACCØRDING TØ ØUTCØME   GMSCT305
C                                                                       GMSCT306
  700 DØ 701 I=1,NSCAT                                                  GMSCT307
  701 YLD(I)=YLDSUM(I)/FLØAT(IHIST)                                     GMSCT308
      CALL SSWTCH(1,K1)                                                 GMSCT309
      IF(K1-2) 702,706,702                                              GMSCT310
  702 WRITE(5,703) IHIST                                                GMSCT311
  703 FØRMAT(5I7)                                                       GMSCT312
      WRITE(5,703) (JNDEX(J),J=1,NSCAT)                                 GMSCT313
      IF(NSCAT-1) 704,705,704                                           GMSCT314
  704 I=NSCAT-1                                                         GMSCT315
      WRITE(5,703) (INDEX(J),J=1,I)                                     GMSCT316
      WRITE(5,703) (NLEV(J),J=1,MNS)                                    GMSCT317
  705 WRITE(5,703) (NHIT(J),J=1,NSCAT)                                  GMSCT318
      WRITE(5,22) (YLD(I),I=1,NSCAT)                                    GMSCT319
  706 CALL SSWTCH(2,K2)                                                 GMSCT320
      IF(K2-1) 707,800,707                                              GMSCT321
  707 IF(IHIST-NHIST) 708,800,800                                       GMSCT322
  708 IHIST=IHIST+1                                                     GMSCT323
      GØ TØ 100                                                         GMSCT324
C                                                                       GMSCT325
C.....END ØF HISTØRY LØØP                                               GMSCT326
C                                                                       GMSCT327
C     FINAL ØUTPUT-IF NSCAT.GT.1 RENØRMALIZE YLD(I) SØ YLD(1)=1 AND     GMSCT328
C     CØMPUTE ALFA                                                      GMSCT329
C                                                                       GMSCT330
  800 WRITE(5,801) IHIST                                                GMSCT331
  801 FØRMAT(10HHISTØRIES=,I8)                                          GMSCT332
      IF(NSCAT-1) 804,804,802                                           GMSCT333
  802 WRITE(5,803)                                                      GMSCT334
  803 FØRMAT(7HNLEV(I))                                                 GMSCT335
      WRITE(5,703) (NLEV(I),I=1,MNS)                                    GMSCT336
  804 WRITE(5,805)                                                      GMSCT337
  805 FØRMAT(7HNHIT(I))                                                 GMSCT338
      WRITE(5,703) (NHIT(I),I=1,NSCAT)                                  GMSCT339
      WRITE(5,806)                                                      GMSCT340
  806 FØRMAT(6HYLD(I))                                                  GMSCT341
      WRITE(5,22) (YLD(I),I=1,NSCAT)                                    GMSCT342
      IF(NSCAT-1) 807,1,807                                             GMSCT343
  807 FYLD=YLD(1)                                                       GMSCT344
      DØ 808 I=1,NSCAT                                                  GMSCT345
  808 YLD(I)=YLD(I)/FYLD                                                GMSCT346
      ALFA=0.0                                                          GMSCT347
      DØ 809 I=2,NSCAT                                                  GMSCT348
  809 ALFA=ALFA+YLD(I)                                                  GMSCT349
      WRITE(5,810)                                                      GMSCT350
  810 FØRMAT(17HNØRMALIZED YLD(I))                                      GMSCT351
      WRITE(5,22) (YLD(I),I=1,NSCAT)                                    GMSCT352
      WRITE(5,811) ALFA                                                 GMSCT353
  811 FØRMAT(5HALFA=,E10.4)                                             GMSCT354
C                                                                       GMSCT355
      IF(K2-1) 1,812,1                                                  GMSCT356
  812 PAUSE                                                             GMSCT357
      GØ TØ 1                                                           GMSCT358
                                                                        GMSCT359
```

```
      END                                                               GMSCT360
      FUNCTIØN DELTA(X0,Y0,Z0,X1,Y1,Z1,X2,Y2,Z2,RS,INDEX)               GMSCT361
C                                                                       GMSCT362
C     FUNCTIØN TØ DETERMINE PENETRATIØN DEPTH FØR R.C. CYLINDER.        GMSCT363
C     INDEX=1,2 ØR 3 IMPLIES CYLINDER AXIS PARALLEL TØ X,Y ØR Z-AXIS    GMSCT364
C     RESPECTIVELY. (X0,Y0,Z0) IS CYLINDER CENTER, (X1,Y1,Z1) IS        GMSCT365
C     EXTERIØR PØINT, (X2,Y2,Z2) IS INTERIØR PØINT, RS=CYLINDER         GMSCT366
C     RADIUS                                                            GMSCT367
C                                                                       GMSCT368
      R=SQRT((X2-X1)*(X2-X1)+(Y2-Y1)*(Y2-Y1)+(Z2-Z1)*(Z2-Z1))           GMSCT369
      A=(X2-X1)/R                                                       GMSCT370
      B=(Y2-Y1)/R                                                       GMSCT371
      C=(Z2-Z1)/R                                                       GMSCT372
      GØ TØ(1,2,3),INDEX                                                GMSCT373
    1 YØW=Y0                                                            GMSCT374
      ZØW=Z0                                                            GMSCT375
      Y1W=Y1                                                            GMSCT376
      Z1W=Z1                                                            GMSCT377
      BW=B                                                              GMSCT378
      CW=C                                                              GMSCT379
      GØ TØ 4                                                           GMSCT380
    2 YØW=Z0                                                            GMSCT381
      ZØW=X0                                                            GMSCT382
      Y1W=Z1                                                            GMSCT383
      Z1W=X1                                                            GMSCT384
      BW=C                                                              GMSCT385
      CW=A                                                              GMSCT386
      GØ TØ 4                                                           GMSCT387
    3 YØW=X0                                                            GMSCT388
      ZØW=Y0                                                            GMSCT389
      Y1W=X1                                                            GMSCT390
      Z1W=Y1                                                            GMSCT391
      BW=A                                                              GMSCT392
      CW=B                                                              GMSCT393
    4 S=(BW*(YØW-Y1W)+CW*(ZØW-Z1W)-SQRT(ABS((BW*BW+CW*CW)*RS*RS-(CW*(Y1WGMSCT394
     1-YØW)-BW*(Z1W-ZØW))*(CW*(Y1W-YØW)-BW*(Z1W-ZØW)))))/(BW*BW+CW*CW)   GMSCT395
      DELTA=R-S                                                         GMSCT396
      RETURN                                                            GMSCT397
      END                                                               GMSCT398
      SUBRØUTINE KINAM(A1,A2,A3,Q,E1,TH3,E31,E32)                       GMSCT399
C                                                                       GMSCT400
      W1=931.478*A1                                                     GMSCT401
      W2=931.478*A2                                                     GMSCT402
      W3=931.478*A3                                                     GMSCT403
      W4=W1+W2-W3-Q                                                     GMSCT404
      EF=-Q*(1.0+(W1/W2)-(0.5*Q/W2))                                    GMSCT405
      EB=-Q*(1.0+(W1/(W2-W3))-(0.5*Q/(W2-W3)))                          GMSCT406
      IF(E1-EF) 1,1,2                                                   GMSCT407
    1 E31=0.0                                                           GMSCT408
   11 E32=0.0                                                           GMSCT409
      GØ TØ 6                                                           GMSCT410
    2 C=CØS(TH3)                                                        GMSCT411
      A=2.0*(W3+W4+E1+Q)                                                GMSCT412
      B=2.0*E1*(W1-W4-Q)-(2.0*W4*Q+Q*Q)                                 GMSCT413
      D=E1*(E1+2.0*W1)*C*C                                              GMSCT414
      TERM=(B*B-2.0*W3*A*B+4.0*W3*W3*D)*E1*(E1+2.0*W1)                  GMSCT415
      IF(TERM) 1,1,3                                                    GMSCT416
    3 DEN=A*A-4.0*D                                                     GMSCT417
      U=(4.0*W3*D-A*B)/DEN                                              GMSCT418
      V=2.0*C*SQRT(ABS(TERM))/DEN                                       GMSCT419
```

```
      E31=U+V                                                                  GMSCT420
      IF(E1-E8) 4,4,5                                                          GMSCT421
    4 IF(TH3-1.5707963) 41,11,11                                               GMSCT422
   41 E32=U-V                                                                  GMSCT423
      GØ TØ 6                                                                  GMSCT424
    5 E32=E31                                                                  GMSCT425
    6 RETURN                                                                   GMSCT426
      END                                                                      GMSCT427
      SUBRØUTINE ANGLE(X1H,Y1H,Z1H,X1T,Y1T,Z1T,X2H,Y2H,Z2H,X2T,Y2T,Z2T,TGMSCT428
     1H)                                                                       GMSCT429
      V1=SQRT(ABS((X1H-X1T)*(X1H-X1T)+(Y1H-Y1T)*(Y1H-Y1T)+(Z1H-Z1T)*(Z1HGMSCT430
     1-Z1T)))                                                                  GMSCT431
      V2=SQRT(ABS((X2H-X2T)*(X2H-X2T)+(Y2H-Y2T)*(Y2H-Y2T)+(Z2H-Z2T)*(Z2HGMSCT432
     1-Z2T)))                                                                  GMSCT433
      DØT=(X1H-X1T)*(X2H-X2T)+(Y1H-Y1T)*(Y2H-Y2T)+(Z1H-Z1T)*(Z2H-Z2T)          GMSCT434
      CTH=DØT/V1/V2                                                            GMSCT435
      TH=ARCCØS(CTH,2)                                                         GMSCT436
      RETURN                                                                   GMSCT437
      END                                                                      GMSCT438
      SUBRØUTINE DISTR(W,TH,V,NW,NMAX)                                         GMSCT439
      DIMENSIØN W(NMAX)                                                        GMSCT440
      V=1,0                                                                    GMSCT441
      IF(NW.EQ.0) GØ TØ 4                                                      GMSCT442
      DØ 2 I=1,NW                                                              GMSCT443
      IF(W(I)) 21,20,21                                                        GMSCT444
   20 VADD=0,0                                                                 GMSCT445
      GØ TØ 22                                                                 GMSCT446
   21 VADD=W(I)*PØLYL(2,I,TH)                                                  GMSCT447
   22 V=V+VADD                                                                 GMSCT448
    2 CØNTINUE                                                                 GMSCT449
      IF(V) 3,4,4                                                              GMSCT450
    3 V=0,0                                                                    GMSCT451
    4 RETURN                                                                   GMSCT452
      END                                                                      GMSCT453
      FUNCTIØN PØLYL(IØP,N,ANGLE)                                              GMSCT454
      X = ANGLE                                                                GMSCT455
      GØ TØ(10,11,12),IØP                                                      GMSCT456
   10 X = .017453293*X                                                         GMSCT457
   11 X = CØS(X)                                                               GMSCT458
   12 NBIG = N-1                                                               GMSCT459
      IF(NBIG) 1,2,3                                                           GMSCT460
    1 PØLYL = 1,0                                                              GMSCT461
      GØ TØ 100                                                                GMSCT462
    2 PØLYL = X                                                                GMSCT463
      GØ TØ 100                                                                GMSCT464
    3 PL = X                                                                   GMSCT465
      PLM1 = 1,0                                                               GMSCT466
      DØ 4 L=1,NBIG                                                            GMSCT467
      PØLYL = (FLØAT(2*L+1)*X*PL - FLØAT(L)*PLM1)/FLØAT(L+1)                   GMSCT468
      PLM1 = PL                                                                GMSCT469
    4 PL = PØLYL                                                               GMSCT470
  100 RETURN                                                                   GMSCT471
      END                                                                      GMSCT472
      SUBRØUTINE INTRPL(N,XT,YT,X,Y)                                           GMSCT473
      DIMENSIØN XT(N),YT(N)                                                    GMSCT474
      IF(X-XT(1)) 1,3,4                                                        GMSCT475
    1 WRITE(1,2)                                                               GMSCT476
    2 FØRMAT(8HRANG ERR)                                                       GMSCT477
      PAUSE                                                                    GMSCT478
    3 Y=YT(1)                                                                  GMSCT479
```

```
      GØ TØ 24                                                          GMSCT480
    4 IF(X-XT(N)) 7,5,1                                                 GMSCT481
    5 Y=YT(N)                                                           GMSCT482
      GØ TØ 24                                                          GMSCT483
    7 I=0                                                               GMSCT484
      J=N                                                               GMSCT485
    8 K=0.5*FLØAT(J-I)+0.1                                              GMSCT486
      K=K+I                                                             GMSCT487
      IF(X-XT(K)) 9,10,11                                               GMSCT488
    9 J=K                                                               GMSCT489
      GØ TØ 12                                                          GMSCT490
   10 Y=YT(K)                                                           GMSCT491
      GØ TØ 24                                                          GMSCT492
   11 I=K                                                               GMSCT493
   12 IF(J-I-1) 13,13,8                                                 GMSCT494
   13 I=J                                                               GMSCT495
      J=I+1                                                             GMSCT496
      DEN=XT(J)-XT(I)                                                   GMSCT497
      C1=(XT(J)*YT(I)-XT(I)*YT(J))/DEN                                  GMSCT498
      C2=(YT(J)-YT(I))/DEN                                              GMSCT499
      Y=C1+C2*X                                                         GMSCT500
   24 RETURN                                                            GMSCT501
      END                                                               GMSCT502
      FUNCTIØN ARCCØS(X,K)                                              GMSCT503
      ARCCØS=1.5707963                                                  GMSCT504
      IF(ABS(X).GT..999999) X=.999999*X/ABS(X)                          GMSCT505
      IF(X*X.GT.1.0E-70) ARCCØS=ATAN(SQRT(ABS(1./X/X-1.)))              GMSCT506
      IF(X.LT.0.) ARCCØS=3.1415926-ARCCØS                               GMSCT507
      GØ TØ (100,200),K                                                 GMSCT508
  100 ARCCØS=ARCCØS*57.2957795                                          GMSCT509
  200 RETURN                                                            GMSCT510
      END                                                               GMSCT511
      FUNCTIØN EXF(Z)                                                   GMSCT512
      IF(Z) 1,1,3                                                       GMSCT513
    1 IF(Z.LT.-70.0) Z=-70.0                                            GMSCT514
      IF(Z.GT.-.1E-04) GØ TØ 2                                          GMSCT515
      EXF=EXP(Z)                                                        GMSCT516
      GØ TØ 4                                                           GMSCT517
    3 IF(Z.GT.70.0) Z=70.0                                              GMSCT518
      IF(Z.LT..1E-04) GØ TØ 2                                           GMSCT519
      EXF=EXP(Z)                                                        GMSCT520
      GØ TØ 4                                                           GMSCT521
    2 EXF=1.0+Z                                                         GMSCT522
    4 CØNTINUE                                                          GMSCT523
      RETURN                                                            GMSCT524
      END                                                               GMSCT525
      SUBRØUTINE FINDI(Y,N,NDIM,Z,IZ)                                   GMSCT526
      DIMENSIØN Y(NDIM)                                                 GMSCT527
      NMIN=1                                                            GMSCT528
      NMAX=N                                                            GMSCT529
   36 INTER=0.5*FLØAT(NMAX-NMIN)+0.1                                    GMSCT530
      NTEST=NMIN+INTER                                                  GMSCT531
      IF(Z-Y(NTEST)) 1,2,3                                              GMSCT532
    1 NMAX=NTEST                                                        GMSCT533
      GØ TØ 4                                                           GMSCT534
    2 IZ=NTEST                                                          GMSCT535
      GØ TØ 999                                                         GMSCT536
    3 NMIN=NTEST                                                        GMSCT537
    4 IF(NMAX-NMIN-1) 5,5,36                                            GMSCT538
    5 IZ=NMAX-1                                                         GMSCT539
```

```
  999 RETURN                                                        GMSCT540
      END                                                           GMSCT541
$                                                                   GMSCT542
```

REFERENCES

1. Donald L. Smith, Report ANL/NDM-12, Argonne National Laboratory (1975).
2. S. A. Cox and P. R. Hanley, IEE Trans. Nucl. Sci. 18, 108 (1971).
3. R. B. Day, Phys. Rev. 102, 767 (1956); Progress in Fast Neutron Physics, edited by G. C. Phillips, J. B. Marion and J. R. Risser (University of Chicago Press, Chicago, 1963).
4. K. Nishimura, K. Okano and S. Kikuchi, Nucl. Phys. 70, 421 (1965).
5. J. B. Parker, J. H. Towle, D. Sams and P. G. Jones, Nucl. Instr. 14, 1 (1961).
6. S. A. Cox, Nucl. Instr. 56, 245 (1967).
7. O. Aspelund and B. Gustafsson, Nucl. Instr. 57, 197 (1967).
8. P. Kuijper, J. C. Veefkind and C. C. Jonker, Nucl. Instr. 77, 55 (1970).
9. W. E. Kinney, Nucl. Instr. 83, 15 (1970).
10. J. K. Dickens, Nucl. Instr. 98, 451 (1972).
11. S. A. Elbakr, I. J. Van Heerden, W. K. Dawson, W. J. McDonald and G. C. Neilson, Nucl. Instr. 97, 283 (1971).
12. B. Minetti and A. Pasquarelli, Nucl. Instr. 120, 509 (1974).
13. E. D. Cashwell, C. J. Everett and O. W. Richards, "A Practical Manual on the Monte-Carlo Method for Random Walk Problems," Report LA-2120, Los Alamos Scientific Laboratory (1957).
14. Evaluated Neutron Data File, ENDF/B-IV, National Neutron Cross Section Center, Brookhaven National Laboratory.
15. E. Storm and H. I. Israel, Nucl. Data Tables A7, 565 (1970).

Table I

Nominal Conditions Considered in Sample Geometry and Absorption Calculations

Geometry:

R_S = 1.9 cm, H = 3.8 cm, D_n = 12.8 cm,

D_γ = 130.0 cm, a = 0.5 cm, various Θ_{DET}

Mesh size:

$n_T = 1$, $n_H = 5$, $n_R = 5$, $n_\phi = 3$

Sample material and gamma ray:

Natural iron, E_γ = 0.846 MeV

Neutron source:

Isotropic yield, Q = 0, $A_1 = 1$, $A_2 = 7$.

Incident energy selected so $E_{n,max}$ = 1 MeV.

Cross sections[a]:

$\Sigma_{nT} = 0.27$, $\Sigma_{\gamma T} = 0.5$

$(d\sigma/d\Omega)_\gamma$ = 0.038 b/sr (isotropic)

Gamma-detector efficiency:

Arbitrary constant value

[a]These are nominal values which are not necessarily equal to ENDF/B-IV values for iron.

Table II

Computed Yield Ratios Which
Demonstrate the Effects of
Geometry and Radiation Absorption

	"Front" - to "back" ratio[a]	"Near" - to "far" ratio[a]
i) Neutron and gamma-ray absorption	2.11	2.11
ii) Gamma-ray absorption only	1.19	2.19
iii) Neutron absorption only	1.78	1.03
iv) No absorption	1.16	1.02

[a] Ratios are defined in Section 3.2.

Table III

Dependence of Gamma-Ray
Yield on the Sample Radius

R_S (cm)	$\bar{Y}_0$ [a]	$R_S\bar{Y}_0$ [a]
0.635	1	1
0.95	0.84	1.25
1.27	0.70	1.41
1.59	0.60	1.50
1.905	0.52	1.55
2.54	0.39	1.57

[a] $\bar{Y}_0$ computed for $\Theta_{DET} = 90°$. Values are relative to corresponding values for $R_S = 0.635$ cm.

Table IV

Nominal Conditions Considered in

Sample Multiple Scattering Calculations

Geometry:

R_S = 1.9 cm, H = 3.8 cm, D_n = 11.4 cm,

D_γ = 130.0 cm, Various θ_{DET}

Sample material and gamma ray:

Natural iron, E_γ = 0.846 MeV

Neutron source:

Isotropic yield, Q = 0, A_1 = 1, A_2 = very large.

Neutron energy E_n = 2 MeV.

Cross sections[a]:

Σ_{nT} = 0.17

Elastic scattering, Q = 0, A_1 = 1, A_2 = 55.85,

Σ_{EL} = 0.17 (isotropic)

Inelastic scattering, Q = -0.85 MeV, A_1 = 1, A_2 = 55.85,

Σ_{IN} = 0.05

$(d\sigma/d\Omega)_\gamma$ = 0.038 b/sr (isotropic)

[a] These are nominal values which are not necessarily equal to ENDF/B-IV values for iron.

Table V

Effect of Coherent Photon Scattering

Sample Material	E_γ (MeV)	Ratio $Y_U/(Y_U + Y_S)$[a]
Li (Z=3)	0.1	1.00
Aℓ (Z=13)	0.1	0.96
	0.3	0.99
	0.5	1.00
Ti (Z=22)	0.1	0.95
	0.3	0.98
	0.5	0.99
	0.8	1.00
Fe (Z=26)	0.1	0.98
	0.3	0.98
	0.5	0.99
	0.8	1.00
Zn (Z=30)	0.1	0.99
	0.3	0.97
	0.5	0.99
	0.8	0.99
	1.0	1.00
Mo (Z=42)	0.1	1.00
	0.3	0.97
	0.5	0.98
	0.8	0.99
	1.0	0.99
	2.0	1.00

[a] Y_U and Y_S are computed using Eqn. (81) and (82). Values of the ratio for larger E_γ are $\sim$ 1.00 if not given in the table.

FIGURE CAPTIONS

Fig. 1. The total cross section for natural iron in the energy range 0.1-2 MeV. The solid curve represents ENDF/B-IV values [14]. The dashed curve represents the same information after smoothing with a 0.1-MeV resolution function. The smoothed excitation function can be approximated by connecting the large dots with straight line segments. This simulates linear interpolation of a lookup table which is stored in the memory of a digital computer. (ANL Neg. No. 116-75-91).

Fig. 2. Schematic diagrams to illustrate geometry applicable to computation of the yield of gamma-rays from (n,Xγ) reactions produced by unscattered neutrons. (ANL Neg. No. 116-75-89).

Fig. 3. Distortion of an isotropic gamma-ray production angular distribution by radiation absorption. (ANL Neg. No. 116-75-85).

Figs.4 thru Fig. 7 Sample midplane relative-yield profiles for the following respective conditions: i) neutron and gamma-ray absorption, ii) gamma-ray absorption only, iii) neutron absorption only, and iv) no absorption. (ANL Neg. Nos. 116-75-84, 116-75-88, 116-75-86, 116-75-82).

Fig. 8. Computed angular resolution functions for several values of Θ_{DET} and Table I parameters. (ANL Neg. Nos. 116-75-80).

Fig. 9. Demonstration of the factorization rule. The solid lines represent assumed differential cross section functions while the solid circles represent values of $\bar{Y}_0/(1 - \Delta\cos\Theta_{DET})$ for various Θ_{DET} but plotted at the corresponding angles $\langle\Theta_{n\gamma}\rangle$. All results are normalized to unity at $\Theta_{DET} = 90°$. (ANL Neg. No. 116-75-87).

Fig.10. Geometry appropriate to multiple-scattering calculations for the first two scattering orders. (ANL Neg. No. 116-75-92).

Fig.11. Plot of relative values for Y_0, Y_1, Y_2 and Y_3 computed using the parameters in Table IV. (ANL Neg. No. 116-75-90).

Fig.12. Plots of α_1, α_2, α_3 and α_{TOT} for various sample sizes ($H = 2\ R_S$). (ANL Neg. No. 116-75-83).

Fig. 13. The relative yield of 0.846-MeV gamma rays per atom for various natural iron samples. Comparison is made between the experimental results and the results of four sets of computations described in Section 5. (ANL Neg. No. 166-75-81).

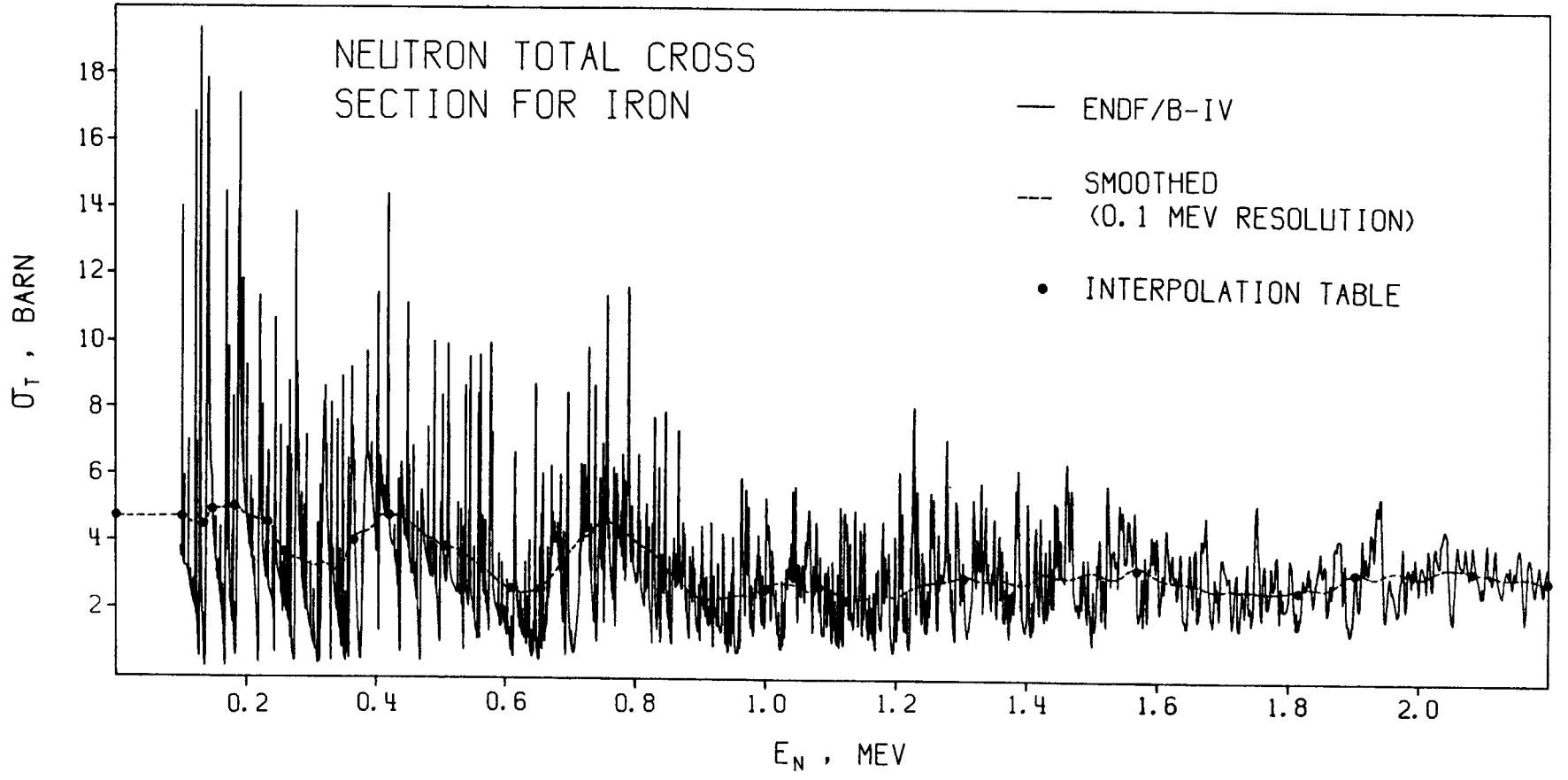
NEUTRON TOTAL CROSS
SECTION FOR IRON
ENDF/B-IV
SMOOTHED
(0.1 MEV RESOLUTION)
INTERPOLATION TABLE
σ_T , BARN
E_N , MEV
18
16
14
12
10
8
6
4
2
0.2
0.4
0.6
0.8
1.0
1.2
1.4
1.6
1.8
2.0

Fig. 1

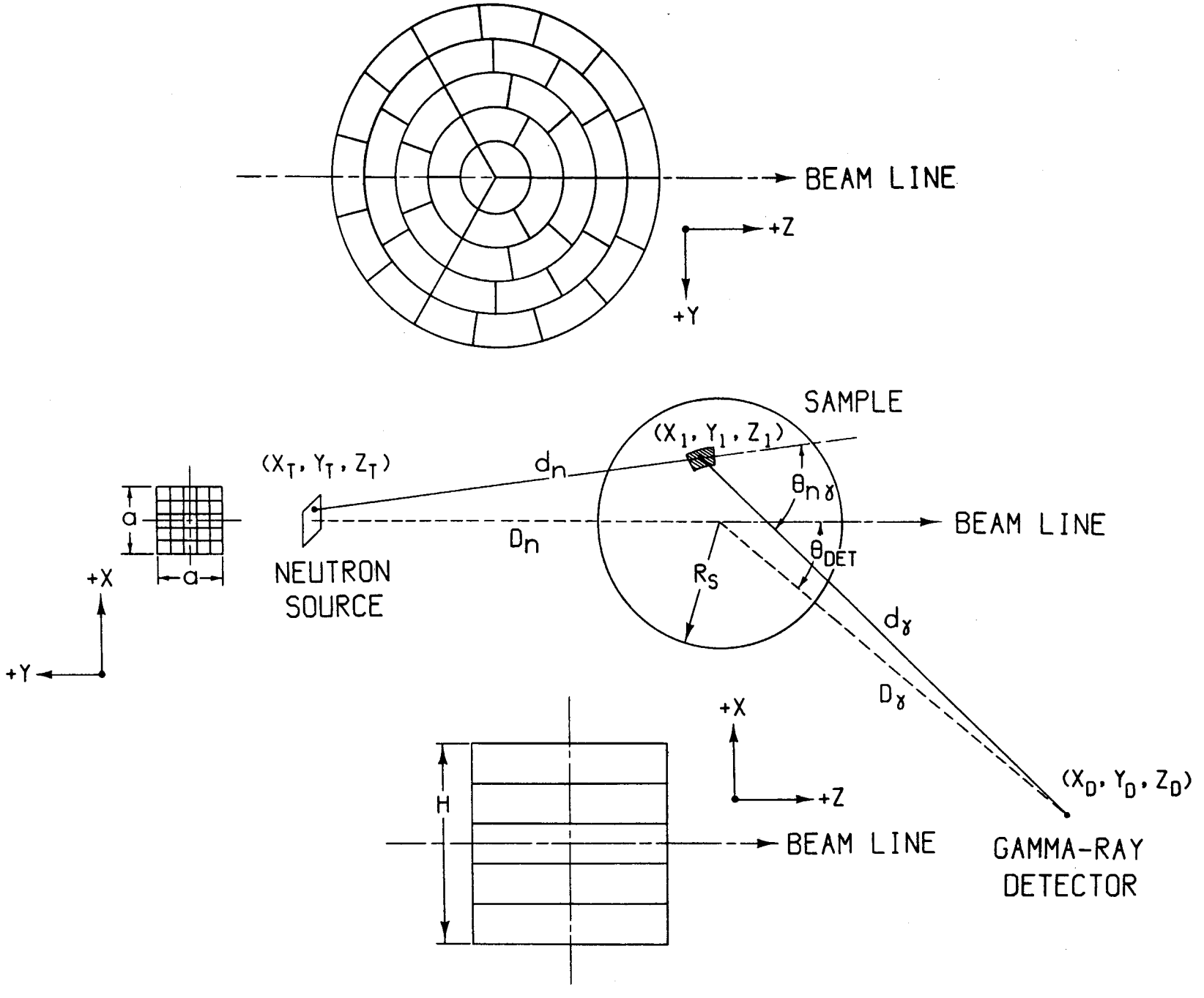
BEAM LINE
+Z
+Y
SAMPLE
(X_1, Y_1, Z_1)
(X_T, Y_T, Z_T)
d_n
$\theta_{n\gamma}$
BEAM LINE
D_n
θ_{DET}
a
a
+X
+Y
NEUTRON SOURCE
R_S
d_γ
D_γ
+X
+Z
(X_D, Y_D, Z_D)
H
BEAM LINE
GAMMA-RAY DETECTOR

Fig. 2

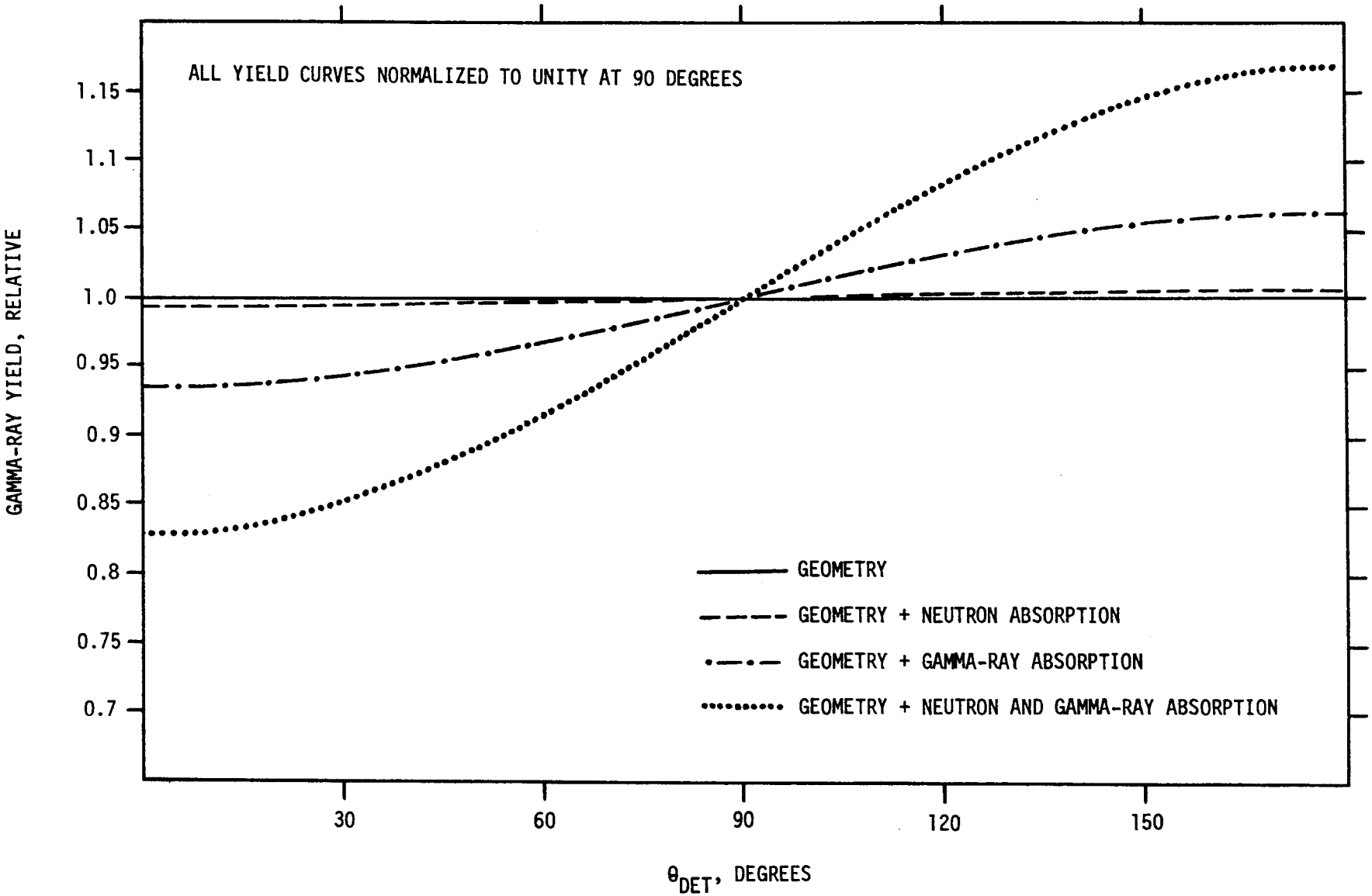
ALL YIELD CURVES NORMALIZED TO UNITY AT 90 DEGREES
GAMMA-RAY YIELD, RELATIVE
1.15
1.1
1.05
1.0
0.95
0.9
0.85
0.8
0.75
0.7
30
60
90
120
150
θDET, DEGREES
GEOMETRY
GEOMETRY + NEUTRON ABSORPTION
GEOMETRY + GAMMA-RAY ABSORPTION
GEOMETRY + NEUTRON AND GAMMA-RAY ABSORPTION

Fig. 3

Fig. 4

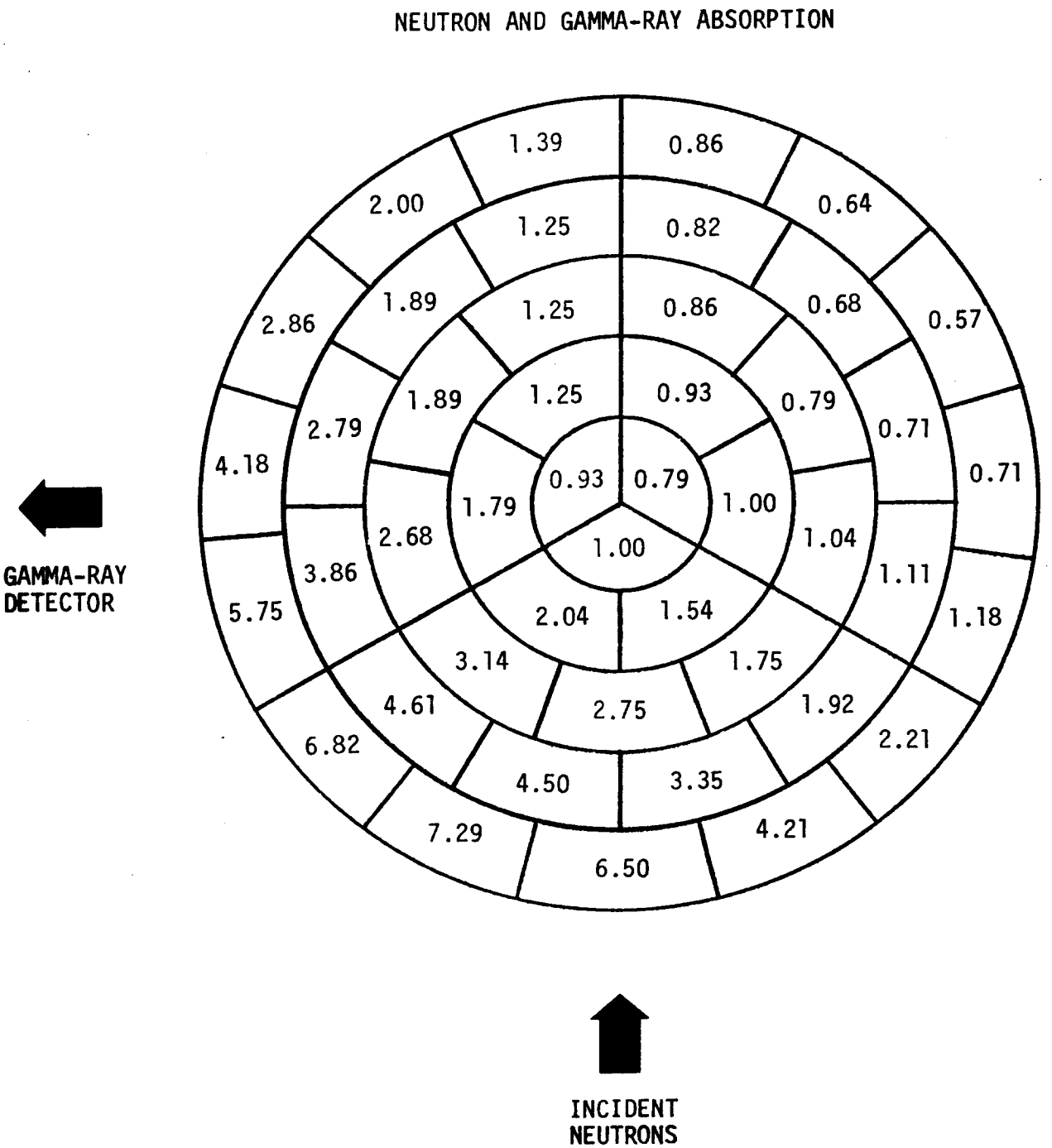
NEUTRON AND GAMMA-RAY ABSORPTION
1.39
0.86
2.00
1.25
0.82
0.64
1.89
1.25
0.86
0.68
0.57
2.86
1.89
1.25
0.93
0.79
0.71
2.79
4.18
0.93
0.79
1.00
0.71
1.79
2.68
1.04
3.86
1.11
1.00
5.75
2.04
1.54
1.18
3.14
1.75
4.61
2.75
1.92
6.82
2.21
4.50
3.35
7.29
4.21
6.50
GAMMA-RAY DETECTOR
INCIDENT NEUTRONS

Fig. 5

GAMMA-RAY ABSORPTION

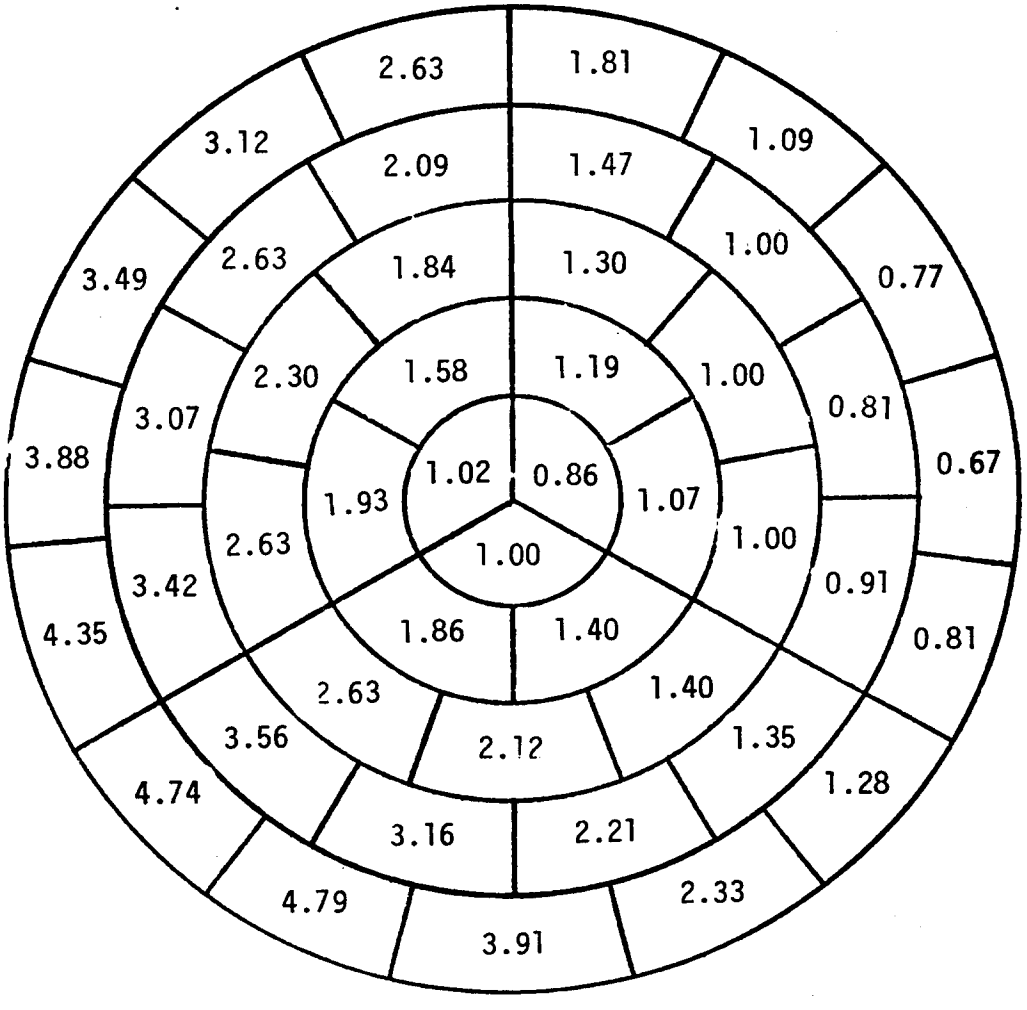

GAMMA-RAY DETECTOR

INCIDENT NEUTRONS

Fig. 6

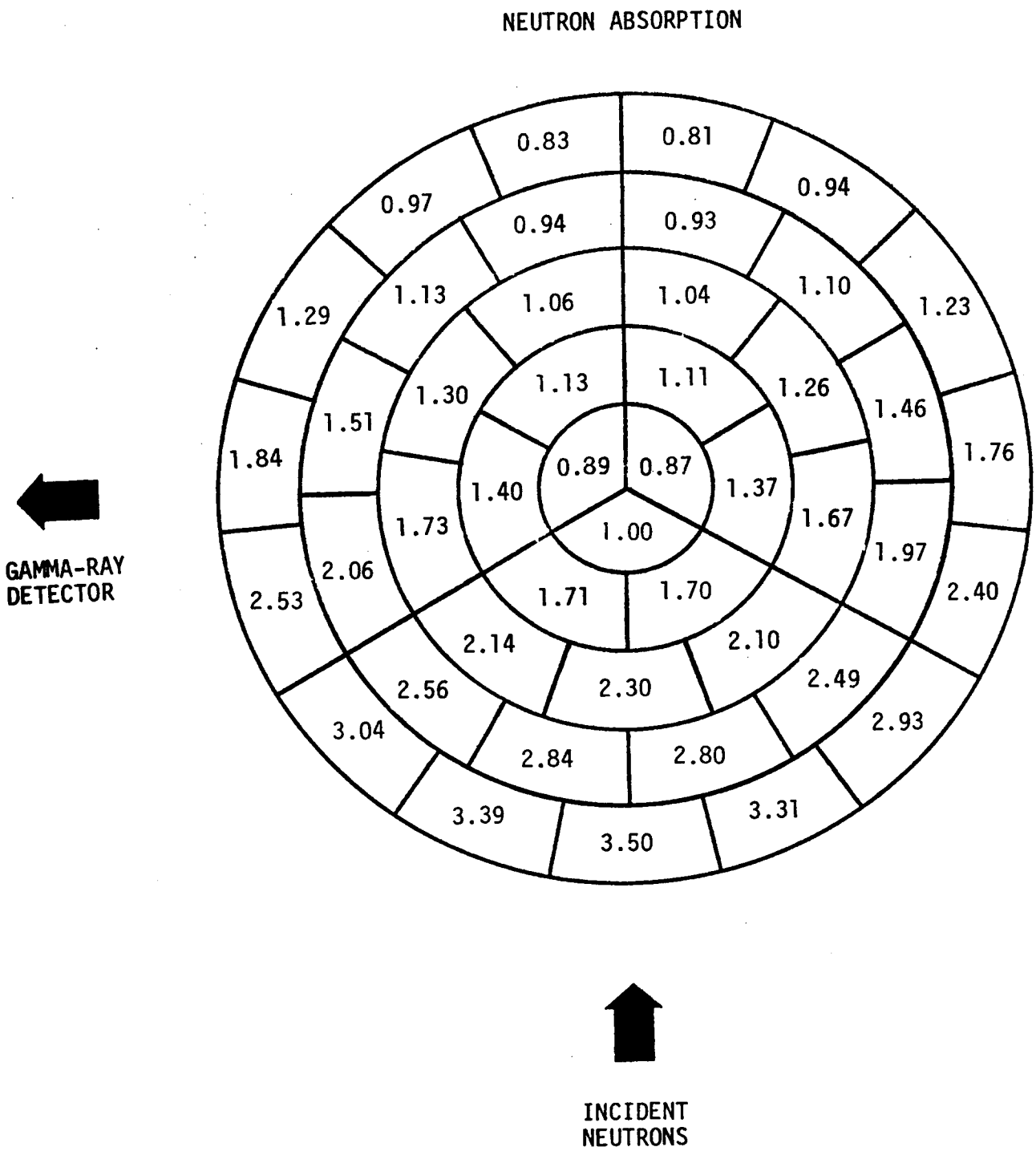
NEUTRON ABSORPTION
0.83
0.81
0.97
0.94
0.94
0.93
1.29
1.13
1.06
1.04
1.10
1.23
1.30
1.13
1.11
1.26
1.46
1.84
1.51
1.76
1.40
0.89
0.87
1.37
1.73
1.00
1.67
1.97
2.06
2.53
1.71
1.70
2.40
2.14
2.10
2.56
2.30
2.49
3.04
2.84
2.80
2.93
3.39
3.31
3.50
GAMMA-RAY DETECTOR
INCIDENT NEUTRONS

Fig. 7

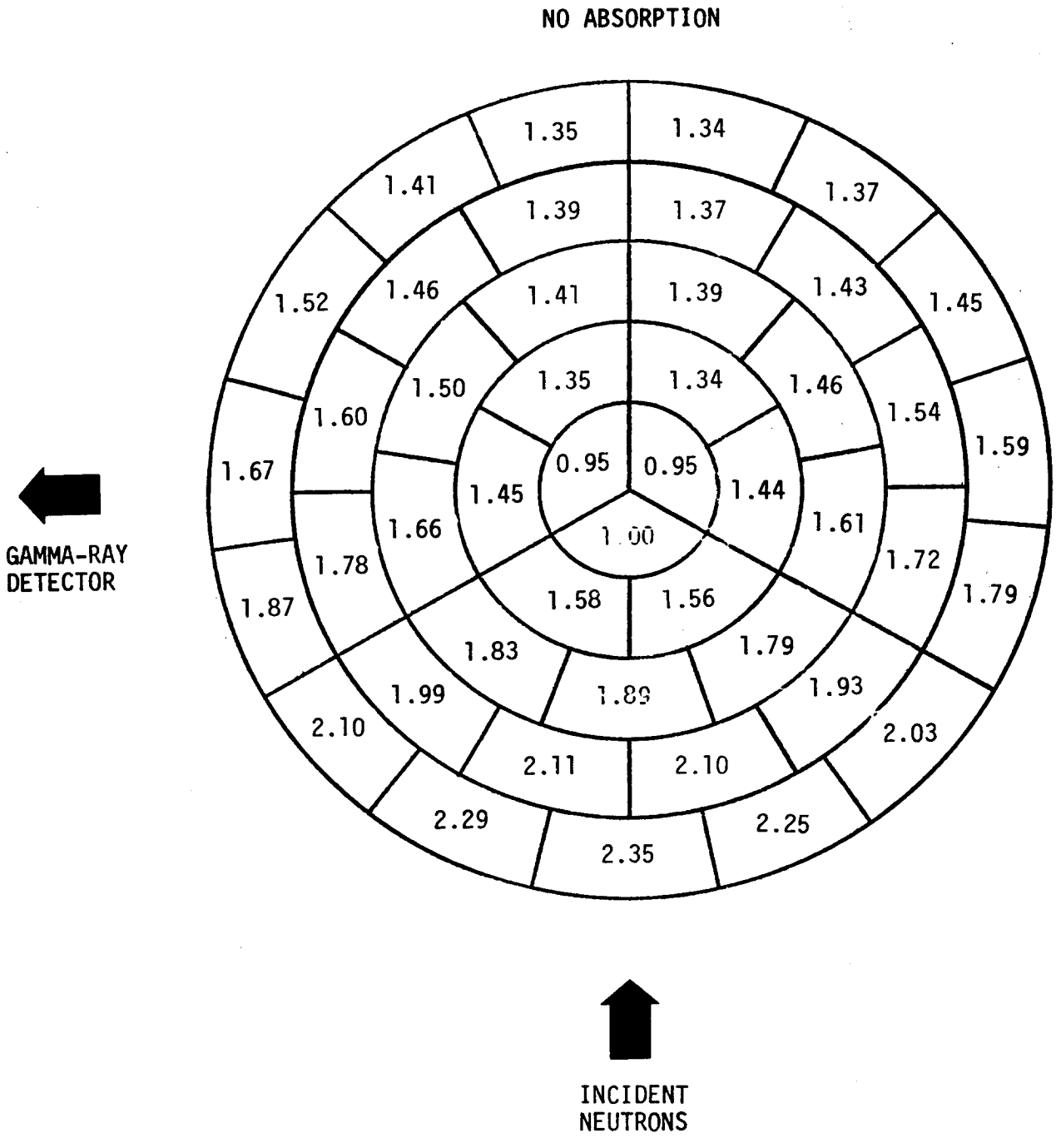
NO ABSORPTION
1.35
1.34
1.41
1.37
1.39
1.37
1.46
1.43
1.45
1.52
1.41
1.39
1.50
1.46
1.54
1.59
1.60
1.35
1.34
1.67
1.45
0.95
0.95
1.44
1.61
1.66
1.00
1.72
1.78
1.79
1.87
1.58
1.56
1.83
1.79
1.93
1.99
1.89
2.03
2.10
2.11
2.10
2.29
2.25
2.35
GAMMA-RAY DETECTOR
INCIDENT NEUTRONS

Fig. 8

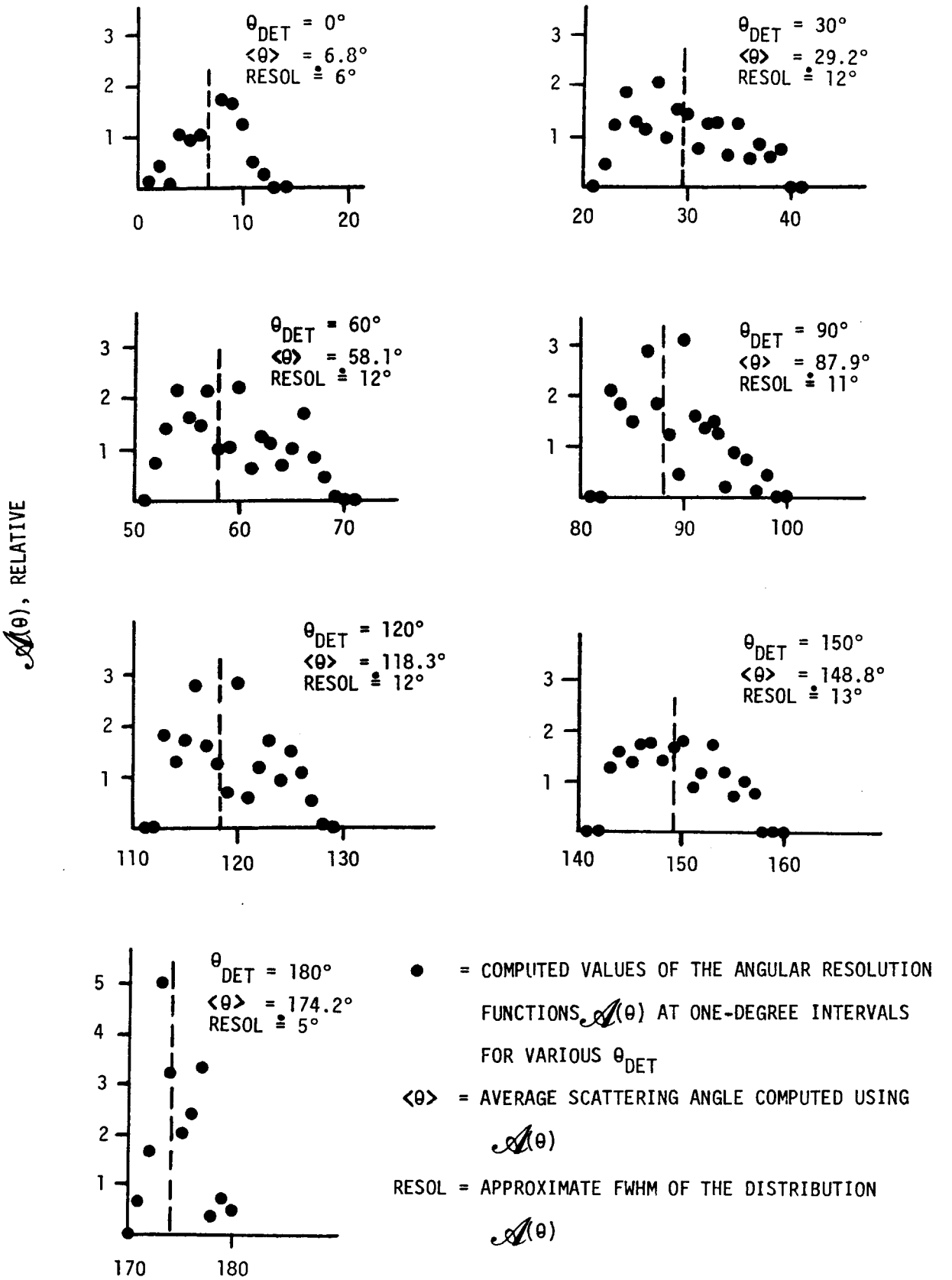

● = COMPUTED VALUES OF THE ANGULAR RESOLUTION FUNCTIONS $\mathscr{A}(\theta)$ AT ONE-DEGREE INTERVALS FOR VARIOUS θ_{DET}

<θ> = AVERAGE SCATTERING ANGLE COMPUTED USING $\mathscr{A}(\theta)$

RESOL = APPROXIMATE FWHM OF THE DISTRIBUTION $\mathscr{A}(\theta)$

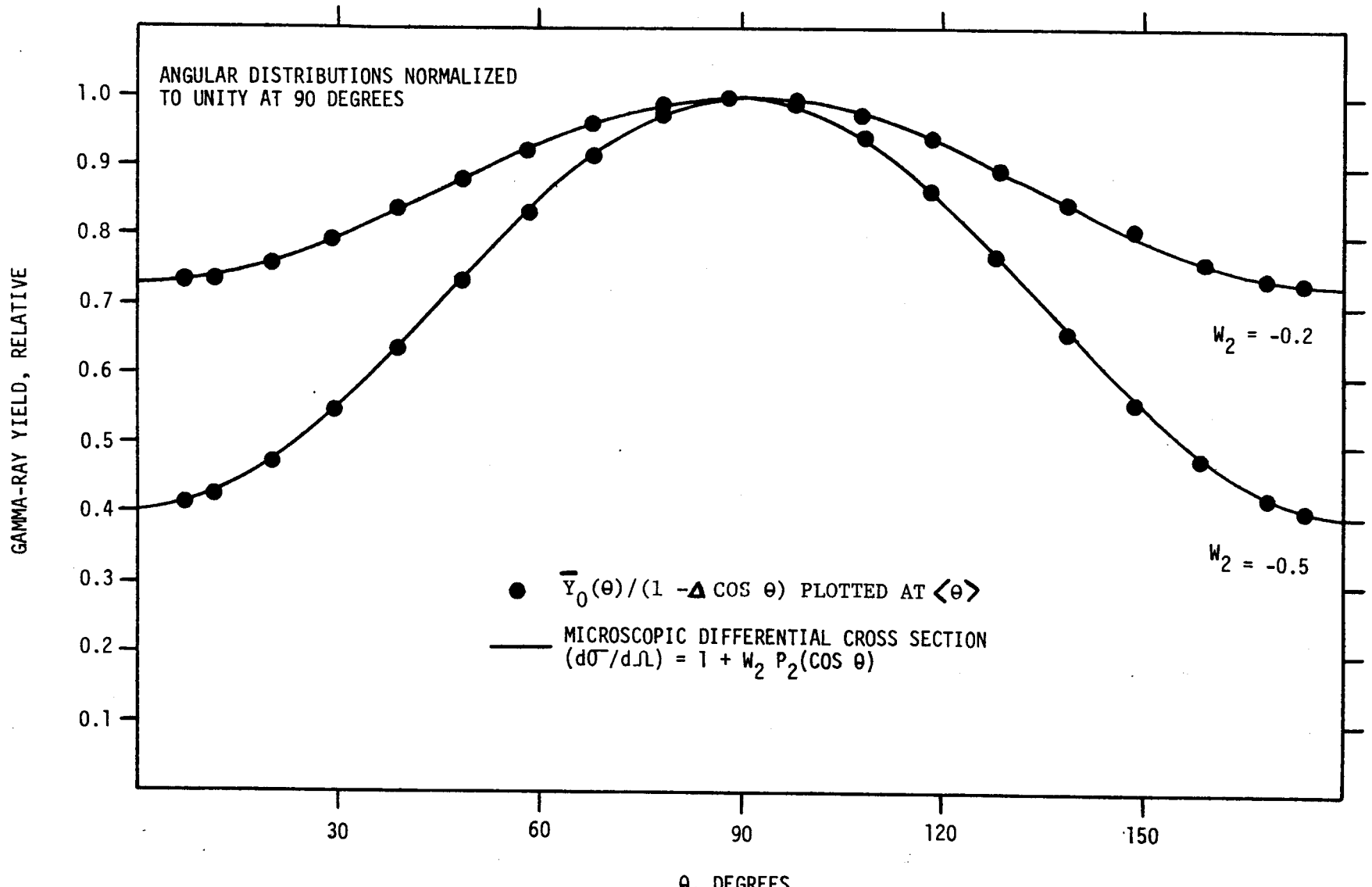
ANGULAR DISTRIBUTIONS NORMALIZED
TO UNITY AT 90 DEGREES
GAMMA-RAY YIELD, RELATIVE
1.0
0.9
0.8
0.7
0.6
0.5
0.4
0.3
0.2
0.1
30
60
90
120
150
θ, DEGREES
W2 = -0.2
W2 = -0.5
Ȳ0(θ)/(1 -Δ COS θ) PLOTTED AT ⟨θ⟩
MICROSCOPIC DIFFERENTIAL CROSS SECTION
(dσ̄/dΩ) = 1 + W2 P2(COS θ)

Fig. 9

Fig. 10

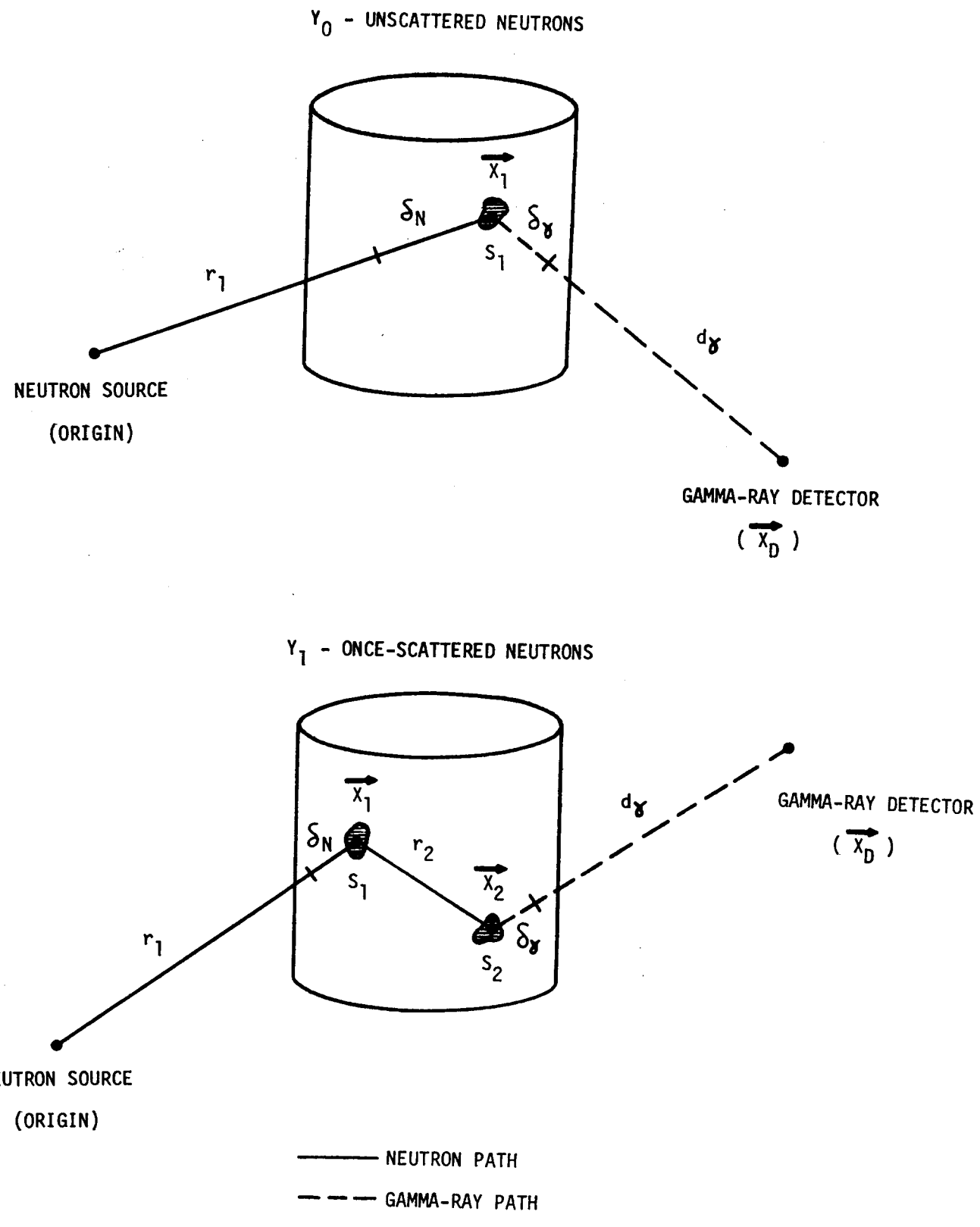
Y_0 - UNSCATTERED NEUTRONS
$\vec{X}_1$
δ_N
δ_γ
S_1
r_1
d_γ
NEUTRON SOURCE
(ORIGIN)
GAMMA-RAY DETECTOR
($\vec{X}_D$)
Y_1 - ONCE-SCATTERED NEUTRONS
$\vec{X}_1$
δ_N
r_2
S_1
$\vec{X}_2$
d_γ
GAMMA-RAY DETECTOR
($\vec{X}_D$)
r_1
δ_γ
S_2
NEUTRON SOURCE
(ORIGIN)
NEUTRON PATH
GAMMA-RAY PATH

Fig. 11

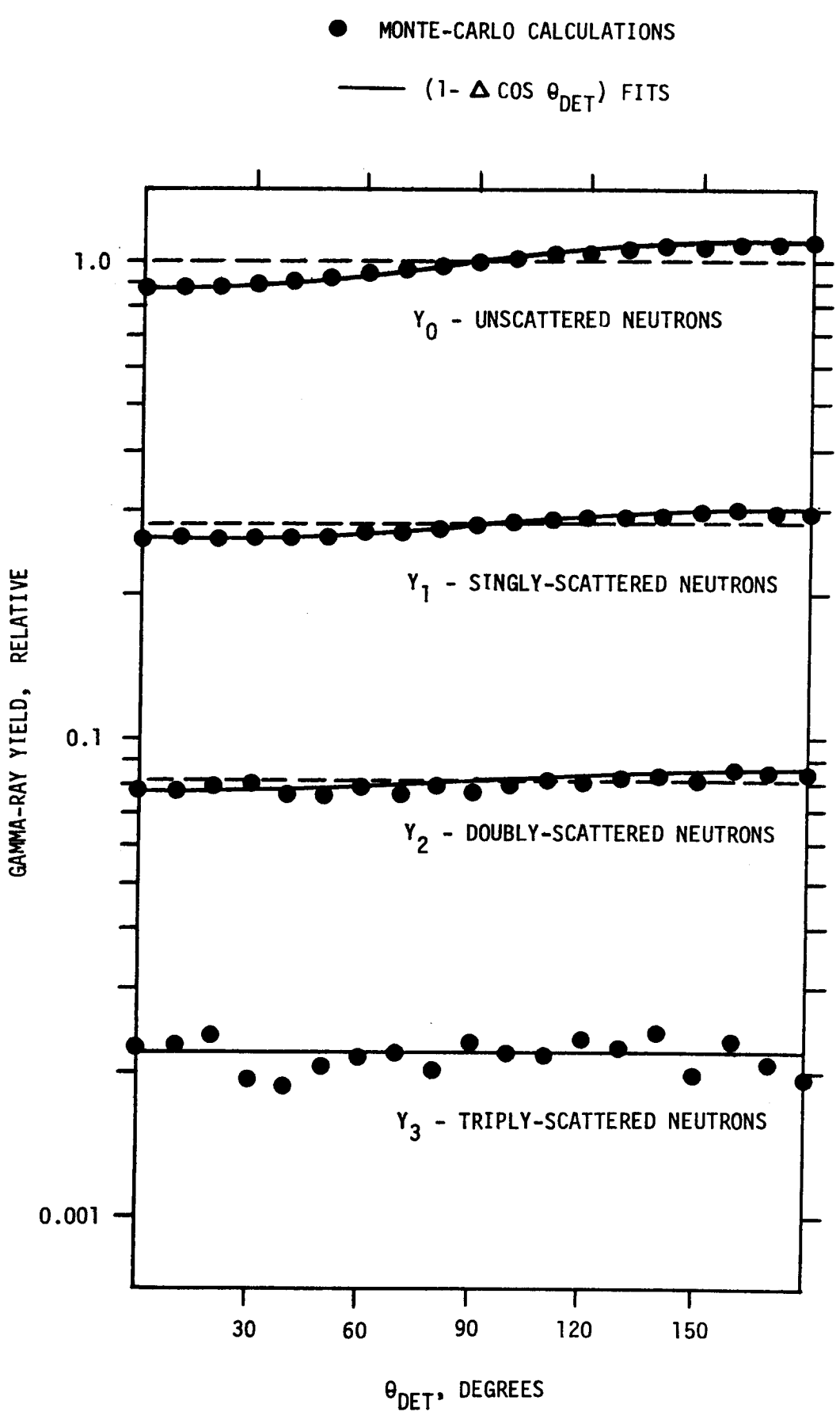
MONTE-CARLO CALCULATIONS
(1- Δ COS θDET) FITS
1.0
0.1
0.001
Y0 - UNSCATTERED NEUTRONS
Y1 - SINGLY-SCATTERED NEUTRONS
Y2 - DOUBLY-SCATTERED NEUTRONS
Y3 - TRIPLY-SCATTERED NEUTRONS
GAMMA-RAY YIELD, RELATIVE
30
60
90
120
150
θDET, DEGREES

Fig. 12

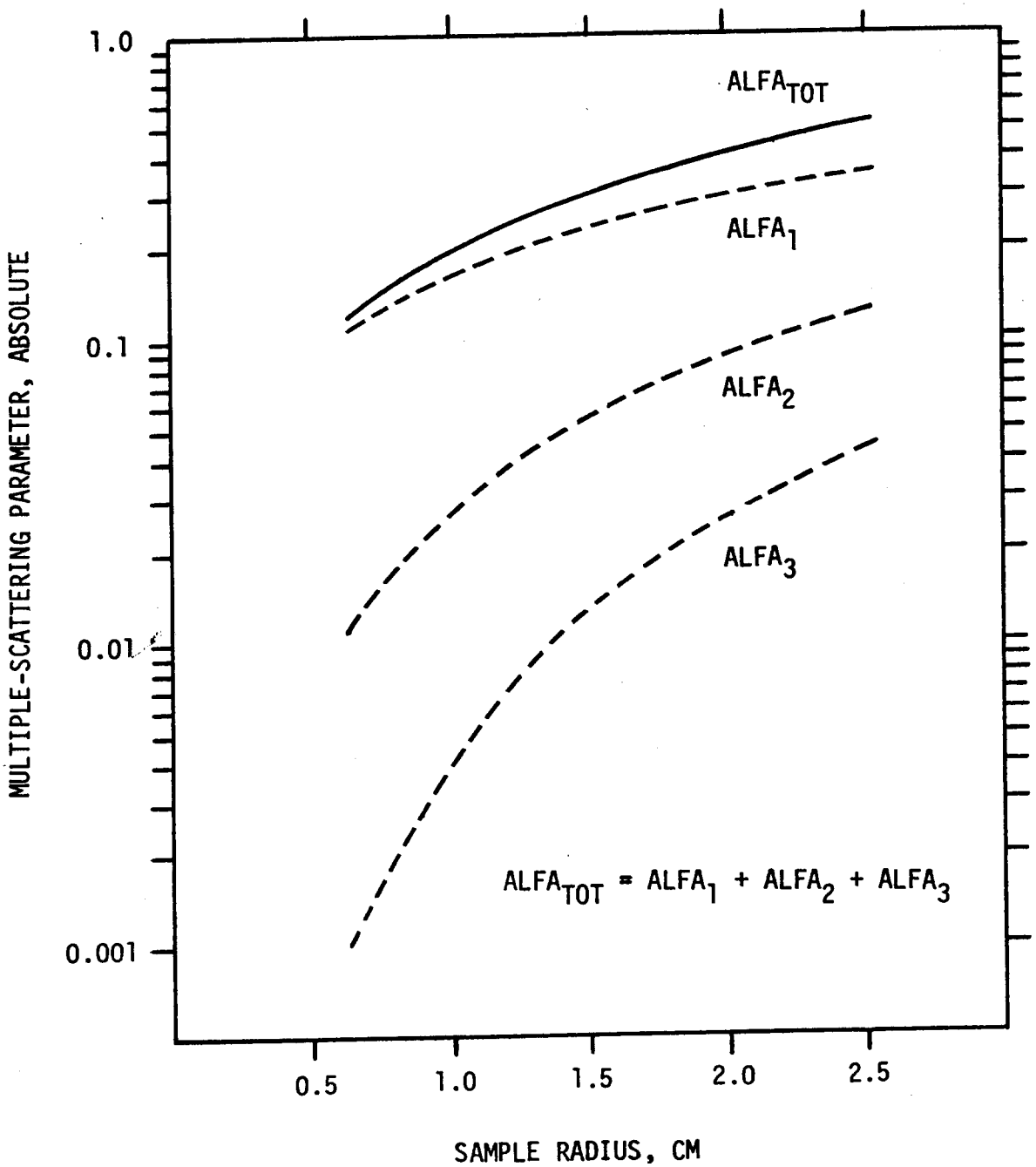
1.0
0.1
0.01
0.001
ALFA$_{TOT}$
ALFA$_1$
ALFA$_2$
ALFA$_3$
ALFA$_{TOT}$ = ALFA$_1$ + ALFA$_2$ + ALFA$_3$
0.5
1.0
1.5
2.0
2.5
MULTIPLE-SCATTERING PARAMETER, ABSOLUTE
SAMPLE RADIUS, CM

Fig. 13

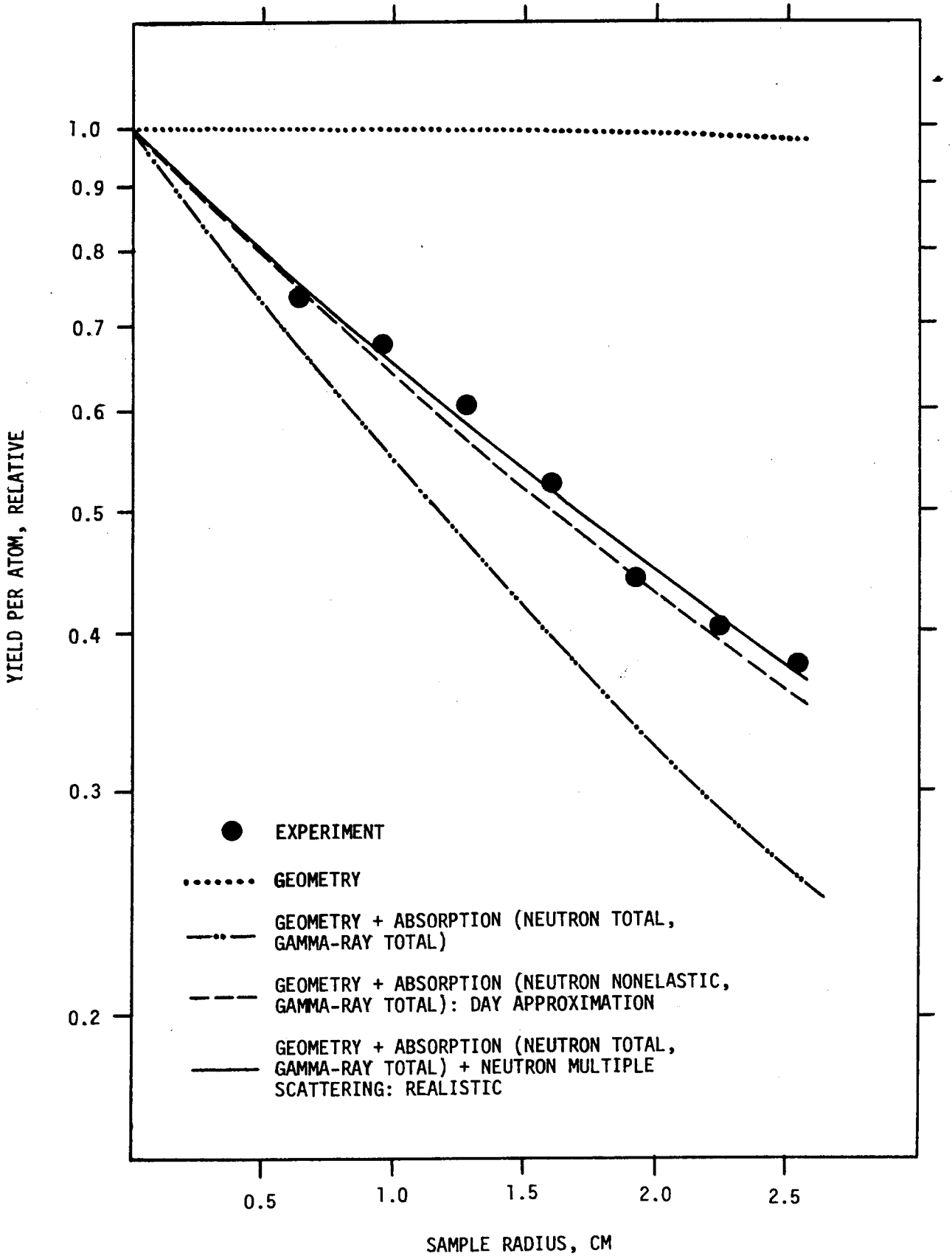
1.0
0.9
0.8
0.7
0.6
0.5
0.4
0.3
0.2
YIELD PER ATOM, RELATIVE
EXPERIMENT
GEOMETRY
GEOMETRY + ABSORPTION (NEUTRON TOTAL, GAMMA-RAY TOTAL)
GEOMETRY + ABSORPTION (NEUTRON NONELASTIC, GAMMA-RAY TOTAL): DAY APPROXIMATION
GEOMETRY + ABSORPTION (NEUTRON TOTAL, GAMMA-RAY TOTAL) + NEUTRON MULTIPLE SCATTERING: REALISTIC
0.5
1.0
1.5
2.0
2.5
SAMPLE RADIUS, CM